

Keratolite–stromatolite consortia mimic domical and branched columnar stromatolites

Jeong-Hyun Lee^{a,*}, Robert Riding^b

^a Department of Geological Sciences, Chungnam National University, Daejeon 34134, Republic of Korea

^b Department of Earth and Planetary Sciences, University of Tennessee, Knoxville, TN 37996, USA



ARTICLE INFO

Keywords:

Cambrian
Keratose sponge
Microbial carbonate
Ordovician
Vermiform fabric

ABSTRACT

The term *keratolite* is proposed for keratosan sponge carbonate dominated by vermicular fabric that preserves the outlines of the original spongin skeleton. Thinly (<~2 cm) interlayered keratosan–microbial carbonate consortia in peritidal sediments near the Cambrian–Ordovician boundary in Newfoundland, Canada, are macroscopically indistinguishable from stromatolites. These carbonate domes and columns consist of approximately equal proportions of keratolite and stromatolite. The keratolite is characterized by pervasive microscopic vermicular fabric, which reflects the original spongin framework. The stromatolite is characterized by fine-grained carbonate with cross-cutting laminae, which primarily formed by sediment trapping. The intimate association of keratolite and stromatolite in these deposits indicates that the sponges and microbes involved shared similar environmental tolerances and requirements. Synchronicity of sponge colonization, followed by stromatolite regrowth, across adjacent columns suggests coordinated responses by both sponges and microbes to local ecophysiological stimuli. Due to their macroscopic similarity, keratolite and fine-grained stromatolite may commonly have been confused with one-another throughout the Phanerozoic, and possibly longer.

1. Introduction

Recognition and definition are recurring themes in microbial carbonate research (Semikhatov et al., 1979; Burne and Moore, 1987; Riding, 1999, 2011; Noffke and Awramik, 2013; Grey and Awramik, 2020; Shapiro and Wilmett, 2020). Early studies struggled with the question of biogenicity (Kalkowsky, 1908; Seward, 1931; Schopf, 2000) and the challenge of distinguishing stromatolites (defined here as laminated benthic microbial deposits; Riding, 1999) from simple animals, such as prokaryotes and sponges (Dawson, 1876, 1896; Walcott, 1895; Wieland, 1914). Progress mainly resulted from comparative studies of present day microbial mat sediments in non-marine and marine environments such as Canandaigua Lake (Walcott, 1914), Andros Island (Black, 1933), and Shark Bay (Logan, 1961). In addition to assisting recognition of ancient examples, these advances stimulated research into microbial communities and the associated processes that localize and precipitate carbonate sediment (Walter, 1976; Monty, 1981; Bertrand-Sarfati and Monty, 1994; Riding and Awramik, 2000; Konhauser, 2006; Reitner et al., 2011).

In this context, the realization that keratosan sponges can mimic stromatolites in macroscopic appearance (Luo and Reitner, 2016) is a

discomfiting development. The composition of the skeletal framework of sponges ranges from CaCO₃ (e.g., Archaeocyatha, Calcarea, Stromatoporidea; Hartman et al., 1980; Senowbari-Daryan and Rigby, 2011) and silica (e.g., Lithistida, Hexactinellida; Hooper and Van Soest, 2002; Reiswig, 2002), to spongin (e.g., Keratosa; Erpenbeck et al., 2012; Reitner and Keupp, 1991; Vacelet, 1991). The original siliceous spicules of hexactinellids and lithistids, as well as the spongin of keratosans, are commonly replaced by CaCO₃ (Warnke, 1995; Luo and Reitner, 2014). Much of the fossil record of these groups resides in carbonate sediments, and it is often possible to distinguish the distinctive outlines and spicular elements of hexactinellids and lithistids in reefal and microbial carbonates (Flügel and Reinhardt, 1989; Leinfelder et al., 1996; Lee et al., 2016a). In contrast, keratosan demosponges preserved in carbonate can be macroscopically indistinguishable from microbial carbonate (Luo and Reitner, 2016).

Here we propose the term keratolite for sediment dominated by the calcified – typically vermicular – remains of keratosan spongin skeleton, and describe examples of intimately interlayered keratolite–stromatolite associations from peritidal carbonates near the Cambrian–Ordovician (485 Myr) boundary in western Newfoundland, Canada. In the field, these sponge–microbial consortia closely resemble branched and

* Corresponding author.

E-mail addresses: jeonghyunlee@cnu.ac.kr (J.-H. Lee), rriding@utk.edu (R. Riding).

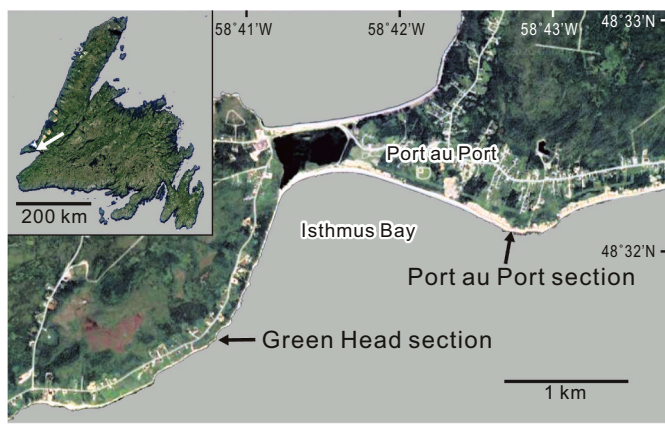


Fig. 1. Location of the study area in western Newfoundland. The Port au Port ($48^{\circ}33'05.8''\text{N}$ $58^{\circ}42'15.9''\text{W}$) and Green Head ($48^{\circ}32'36.8''\text{N}$ $58^{\circ}44'12.5''\text{W}$) sections are located on the eastern and western sides of Isthmus Bay, respectively. Modified from [Google \(2020\)](#).

dome-shaped stromatolites, casting doubt on the ability of meso-macroscopic (e.g., field-based) studies, on their own, to confidently recognize fine-grained stromatolites (Reitner et al., 1995). This supports the troubling realization that – even though *bona fide* Phanerozoic stromatolites

are well-documented – keratosan-microbial consortia could have been mistaken for stromatolites throughout the Phanerozoic (Luo and Reitner, 2016), and possibly also in the late Proterozoic, since it is widely thought that sponges – including keratosans – could have originated in the Neoproterozoic (Wörheide et al., 2012; Sperling and Stockey, 2018). On a more positive note, keratosan–microbial consortia demonstrate that metazoan–mat relationships were not exclusively competitive, and that these groups could cooperate in building calcified benthic communities (Luo and Reitner, 2016; Lee and Riding, 2021).

2. Geological setting

Upper Cambrian–Lower Ordovician shallow marine carbonates are common along the eastern margin of Laurentia (Kennard and James, 1986; Pratt and James, 1986; James et al., 1989; Kennard et al., 1989; de Freitas and Mayr, 1995; Stouge et al., 2001; Lavoie et al., 2012; Lavoie, 2019, fig. 6). In western Newfoundland, this succession is well exposed in coastal sections on the south-eastern side of the Port au Port Peninsula and immediately to the east along the shores of Isthmus Bay, ~10 km west of Stephenville (Williams et al., 1985). The upper Cambrian (Stage 10, Furongian) and lowermost Ordovician Berry Head Formation, at the top of the Port au Port Group, is overlain by the Lower Ordovician (Tremadocian) Watts Bight Formation, at the base of the St George Group (Knight et al., 2008, fig. 2; Scorrer et al., 2019, fig. 2). On the

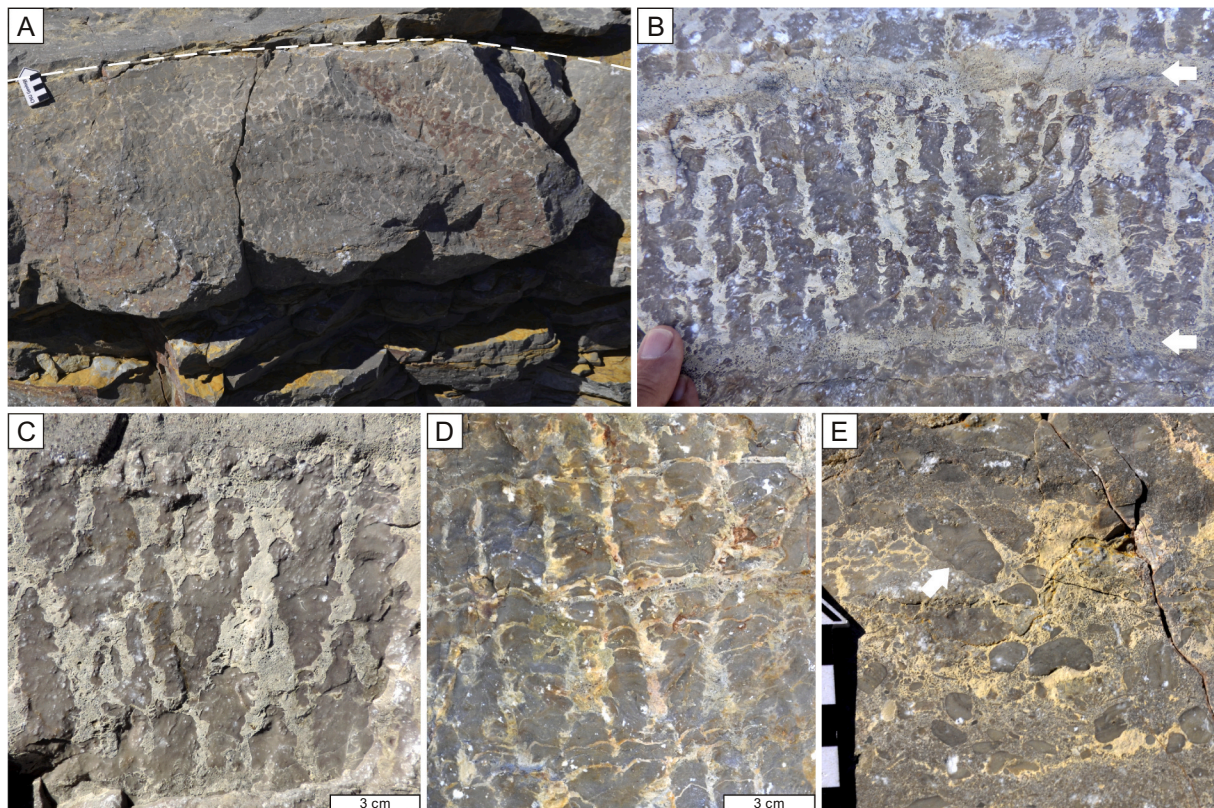


Fig. 2. Branching keratolite–stromatolite columns; uppermost Cambrian (Berry Head Formation), Port au Port section. Location, see Fig. 1. (A) Numerous columns form a broad low dome, 2–3 m wide and 60–70 cm thick, underlain by thin-bedded lime mudstone and overlain by rudstone which also occurs lateral to the dome. Cm scale. (B) Erect columns surrounded by light-gray coarse dolomitic matrix, which also forms layers above and below the columns (arrows). (C) Divergent, upward-widening columns with coarse sediment layers at base and top. (D) Densely packed columns with thin layers of coarse sediment that cross the columns. (E) Broken column fragments (large example arrowed) in adjacent rudstone. Cm scale.

eastern side of Isthmus Bay, conodont studies locate the Cambrian–Ordovician boundary at a conformable contact ~16 m below the base of the Watts Bight Formation (Scorger et al., 2019, fig. 8). The Cambrian–Ordovician succession in this area corresponds to a major unconformity further west (Lavoie et al., 2012; Lavoie, 2019). Berry Head–Watts Bight sediments are dominated by fine-grained, often burrowed, peritidal carbonates with intraclastic sand and rudstone horizons (Knight et al., 2008). Thrombolites and putative stromatolites are common (Kennard and James, 1986; Pruss and Knoll, 2017) and locally form Lower Ordovician mounds in association with sponges (*Archaeoscyphus*, *Pulchrilamina*), sponge-like organisms (*Calathium*) and *Amsasia* (Pratt and James, 1982, 1989a; Knight and James, 1987; Knight et al., 2008; Elias et al., 2021).

3. Field descriptions

We collected putative stromatolites (which we now recognize as keratolite–stromatolite consortia) from the uppermost Cambrian (Berry Head Formation) and lowermost Ordovician (Watts Bight Formation; ~485 Ma) successions in coastal exposures on the eastern and western sides of Isthmus Bay (Fig. 1). These localities were respectively named Port au Port and Green Head by Ji and Barnes (1994).

3.1. Locality 1, Port au Port (uppermost Cambrian, Berry Head Fm.)

A ca. 200 m thick northward-younging Cambrian–Ordovician boundary succession is exposed along the eastern shore of Isthmus Bay, south and southeast of Port au Port (Fig. 1). This section has also been referred to as East Isthmus Bay (Scorger et al., 2019, fig. 1). Our sample horizon is ~30–33 m below the top of Berry Head Formation, and ~14–17 m below the Cambrian–Ordovician boundary, corresponding to thickness level 133–130 m of Scorger et al. (2019, fig. 3).

We sampled branched columns that form broad low domes, up to ~1 m thick and a few meters wide, overlying thin bedded lime mudstone (Fig. 2A) and laterally surrounded by intraclastic rudstone. The rudstones contain surrounded pebbles that include reworked columns, 1–3 cm in size, indicating synsedimentary lithification of the columns (Fig. 2E). The columns in the domes are 1–2 cm wide, short (~2–4 cm high), erect, closely spaced, and irregularly branched, with margins that can be smooth but are more commonly irregular. Their convex-up laminae indicate relatively low primary relief. Adjacent columns occur in subhorizontal horizons 5–10 cm thick, separated by thin (~1 cm) layers of medium to coarse intraclastic packstone-grainstone (Fig. 2B–D). Similar sediment occupies intercolumn spaces. The columns often widen upward, and locally show bridging. Their margins are commonly ornamented by irregular lateral projections and protrusions (Fig. 2C). Branching ranges from parallel to slightly divergent (see Walter, 1972, fig. 3), primarily in response to influx of carbonate sediment. In overall appearance, these branched columns broadly resemble stromatolites that were widespread in the Neoproterozoic, ~800 Ma (e.g., Walter, 1972; Grey and Blake, 1999, fig. 6; Grey and Awramik, 2020, fig. 94a, d). The immediately associated sequence includes small steep-sided putative stromatolite domes with up to 15 cm of primary relief, thrombolite domes, and carbonates ranging from locally bioturbated thinly bedded micrite to coarse intraclastic rudstone (Scorger et al., 2019, fig. 3) and flat pebble conglomerate. These deposits suggest shallow water environments in which sediments were commonly reworked by waves and currents. Skeletal fossils are scarce in the sampled horizon, but brachiopods, trilobites and conodonts in the

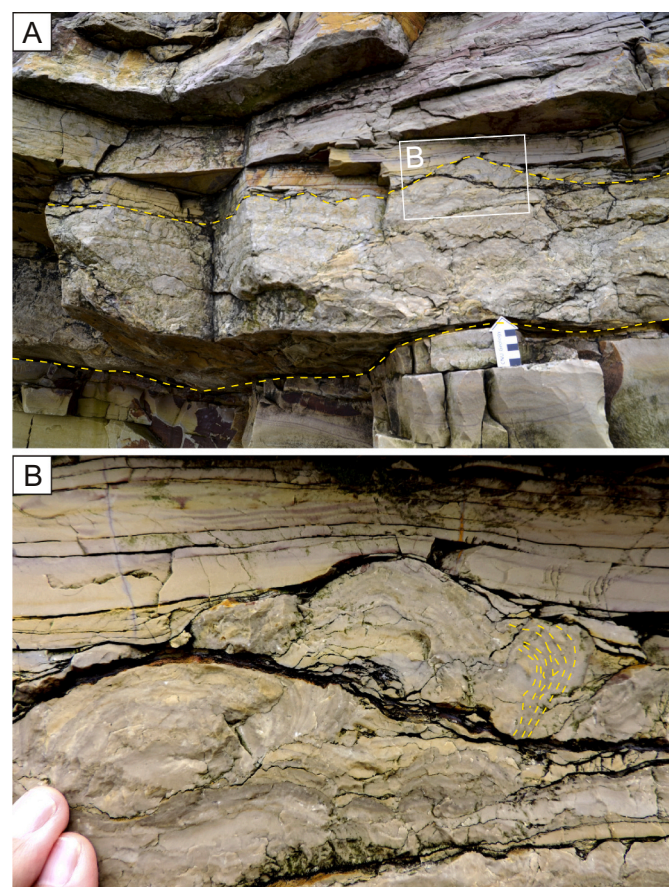


Fig. 3. Domical keratolite-stromatolite, lowermost Ordovician (Watts Bight Formation), Green Head section. Location, see Fig. 1. (A) Biostrome (dashed outline) of small keratolite-stromatolite domes, underlain and overlain by fine-grained tan colored carbonate. Cm scale. (B) Detail of (A) showing domes with steep to over-hanging margins (dotted lines).

associated succession (Scorger et al., 2019) indicate normal marine salinity.

3.2. Locality 2, Green Head (lowermost Ordovician, Watts Bight Fm.)

This northward-younging Cambrian–Ordovician boundary succession is exposed in coastal cliffs along the western side of Isthmus Bay, southwest of Port au Port (Fig. 1). It comprises sections termed Green Head (Pratt and James, 1982, fig. 2 and p. 558; Ji and Barnes, 1994, fig. 1) and Isthmus Bay (Pratt and James, 1986, fig. 2; Knight et al., 2008, fig. 3), as well as the Watts Bight and Boat Harbour reference sections of Knight and James (1987, fig. 3d). Our samples are early Tremadocian in age. They overlie thrombolite mounds with abundant chert nodules, ~5 m above the base of the Watts Bight Formation (Knight et al., 2008, fig. 4 column B).

We sampled a horizon of small, pale tan colored, planar to laterally linked low domes, in beds up to ~20 cm thick. Individual domes, ~5 cm wide with ~2–3 cm of primary synoptic relief, are underlain and overlain by bedded micrites (Fig. 3A). Samples were collected from the uppermost part of the bed, where thinly bedded micrite onlaps the domes (Fig. 3B). The immediately associated sequence includes laminated lime

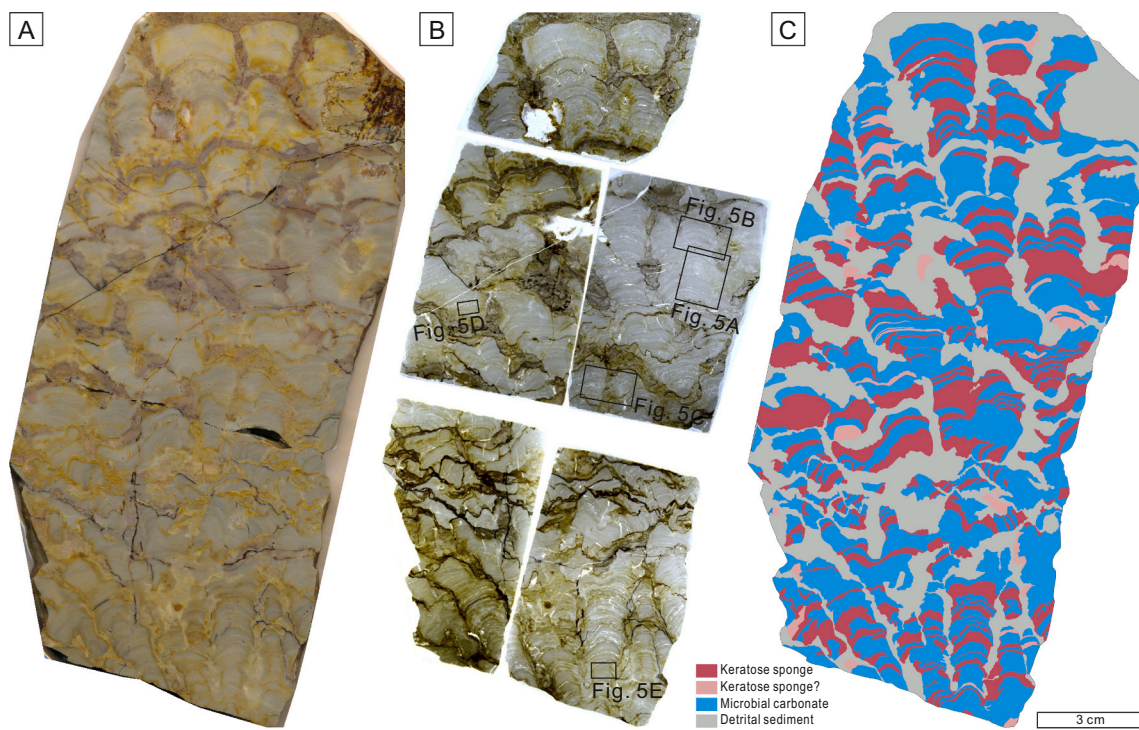


Fig. 4. Columnar branching keratolite-stromatolite; Port au Port section. (A) Vertical slab. (B) Thin-sections of the slab, showing positions of the photomicrographs shown in Fig. 5. (C) Map showing keratosan sponge (keratolite) and microbial carbonate (stromatolite). Both form relatively even alternating layers, mostly up to ~2 cm thick, that tend to persist laterally across adjacent columns.

mudstones and bioturbated dolostones with abundant thrombolite mounds (Knight et al., 2008). A horizon of microbial domes with chert linings, slightly lower in the sequence, marks the base of the Watts Bight Formation (Knight et al., 2008). The “Green Head Mound Complex”, with thrombolite and *Amsussia* (Pratt and James, 1982; Elias et al., 2021), occurs ~20 m above the sampled horizon. The overall depositional environment of the Watts Bight Formation has been interpreted as peritidal (Pratt and James, 1986). Macrofossils are generally scarce (Knight et al., 2008).

4. Slab and thin section descriptions

4.1. Port au Port branched columns

The keratolite-stromatolite columns either maintain their width vertically or, more commonly, slowly expand upward. They are generally closely spaced, and typically equal or exceed the volume of intercolumn sediment (Fig. 4). Each column consists of regular to irregular alternations of keratosan sponge and microbial carbonate (Figs. 4, 5). The overall ratio of keratolite to microbial carbonate is 38% to 62% (Fig. 4C). Branching appears unrelated to whether the column is dominated by keratolite or microbial carbonate at the point of branching, and bridges that connect the columns can be formed by keratolite and/or microbial carbonate (Fig. 5C). Intercolumn matrix is dominated by subrounded-angular fine to coarse intraclast packstone-grainstone (Fig. 5A–C), locally with small column fragments, and is commonly dolomitized (Fig. 4A, B).

The keratolite layers can be exceedingly thin, and typically range

~1–10 mm in thickness. They are characterized by pervasive “vermiciform” fabric: microscopic sparry networks that traverse micritic groundmass (Fig. 5A–D; see Section 5.3. Vermiform fabric, below). Keratolite layers generally maintain their millimetric thickness across the column width, which is typically ~1–4 cm, and can often be traced at the same level from column to column across entire hand samples (~10 cm; Figs. 2B–D, 4). These layers tend to have relatively even, well-defined bases, with slightly to moderately irregular – often less well-defined – tops (Fig. 5A, B). Correspondingly, microbial carbonate layers have slightly to moderately irregular bases, and relatively even tops. Small scale lateral interfingering occurs locally between sponge and microbial carbonate (Fig. 5A, B).

Preservation is generally good in both microbial and keratosan fabrics, consistent with synsedimentary lithification, and the columns are only slightly dolomitized. In shape and size, the outlines of these Port au Port keratosan sponges closely resemble those of some present-day examples (e.g., Luo and Reitner, 2016, fig. 6F). Microbial fabrics show both even and cross-cutting fabrics (Fig. 5E) and locally incorporate carbonate silt-sand grains (e.g., lower part of Fig. 5A), suggesting agglutination of allochthonous sediment. Nonetheless, adjacent reworked keratolite-stromatolite clasts (Fig. 2E) also indicate synsedimentary lithification.

4.2. Green head domes

These small, laterally linked (see Logan et al., 1964) and well-laminated keratolite-stromatolite domes, with locally steeply angled margins, occur within sand-poor, very fine-grained, carbonate

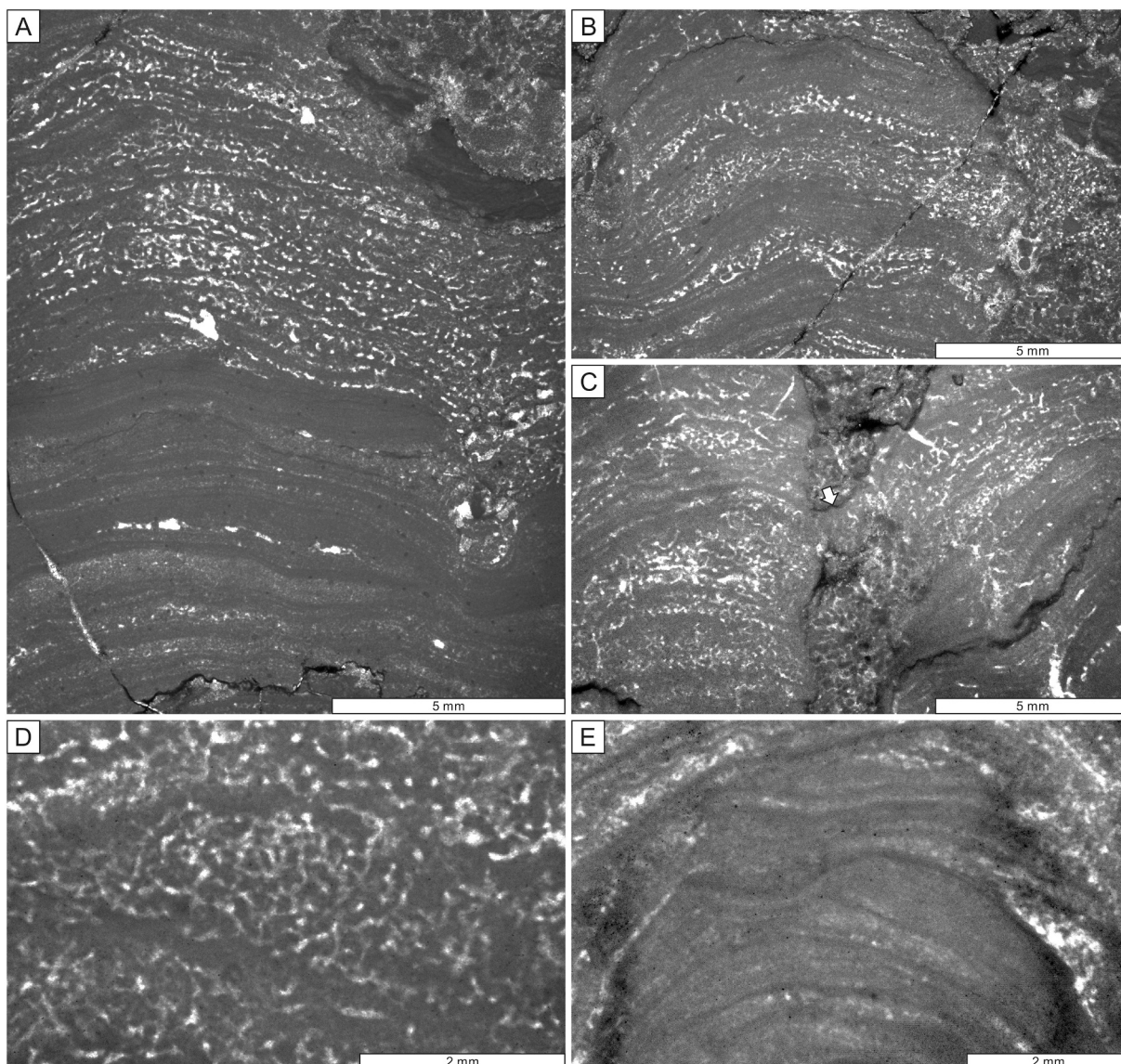


Fig. 5. Photomicrographs of columnar keratolite–stromatolite; Port au Port section. See positions of thin-sections in Fig. 4B. (A) Stromatolite (lower part) overlain by vermiciform keratolite sponge (keratolite; upper part). Both show lamination, which is more delicate in the stromatolite. (B) Thinly interlayered keratolite–stromatolite column. (C) Adjacent columns separated by intraclastic grainstone but connected by a sponge (keratolite) bridge (arrow). (D) Detail of keratolite sponge (keratolite) showing characteristic vermicular fabric produced by the original spongin fiber network. (E) Detail of stromatolite column, showing cross-cutting laminae suggestive of sediment trapping associated with current transport. Keratolite sponge (vermicular fabric; keratolite) occurs at the sides and top.

mudstones (Fig. 3B). The keratolite–microbial carbonate ratio within the mapped domes is equal (50:50; Fig. 6C), and overall layer thicknesses, as well as the internal structures of both the keratosan sponges and the microbial carbonates, are similar to those of Port au Port columns (Fig. 7). The fine-grained micritic microbial carbonate is dominated by well-defined uneven laminae that commonly show cross-cutting (Fig. 7). Allomicrite layers are commonly intercalated with sponge/microbial carbonate layers (Figs. 6, 7B). The keratolite layers range from very thin to 5 mm thick. They have smooth bases, but the tops can be even more irregular (Figs. 6, 7A) than those of the Port au Port columns, and small, isolated growths surrounded by allomicrite occur locally (Fig. 7B).

4.3. Comparisons

The branched columns (Port au Port) and small domes (Green Head) are both macroscopically laminated. Microscopically they consist of interlayered keratolite sponge (keratolite) and microbial carbonate (stromatolite). Each of these components tends to form discrete laterally persistent bands that alternate with one-another on mm–cm scales. The matrix is coarse in the Port au Port samples, and fine in the Green Head samples. Nonetheless, these domes and branches both contain roughly similar proportions of keratolite and stromatolite. In both cases, the keratolite is dominated by vermicular microfabric and the stromatolite is typically finely layered micrite with thin, cross-cutting laminae that

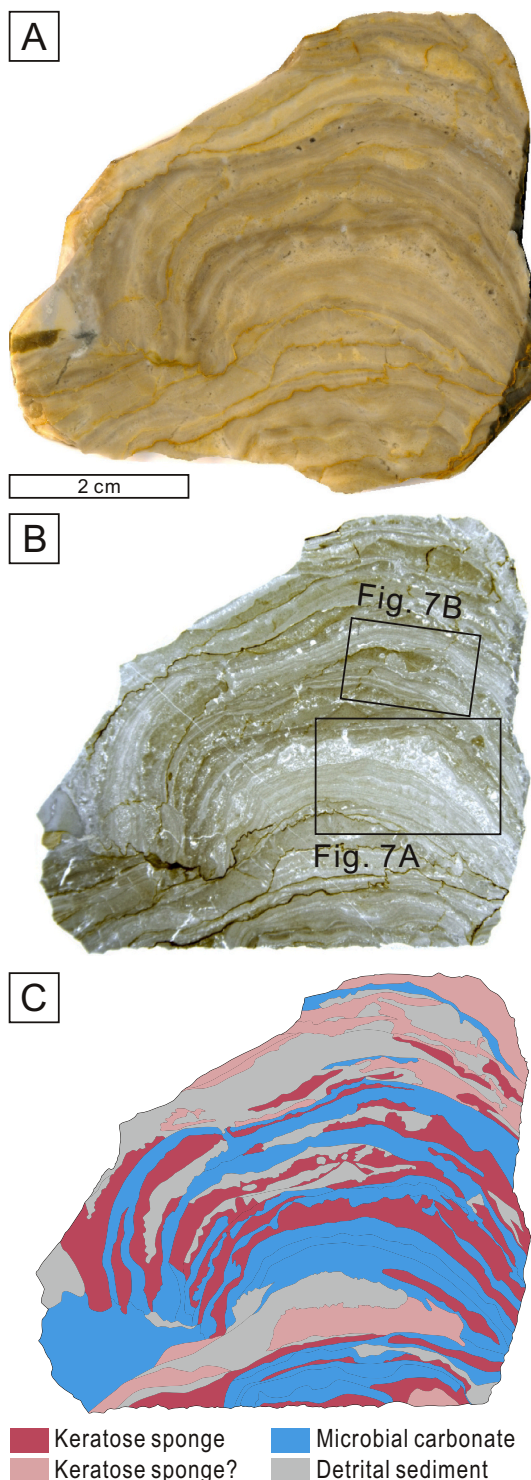


Fig. 6. Domical keratolite-stromatolite with steep margins; Green Head section. (A) Vertical slab. (B) Thin-section of the slab, showing positions of the photomicrographs in Fig. 7. (C) Map showing keratosan sponge (keratolite) and microbial carbonate (stromatolite). Both components form irregular alternating layers up to ~1 cm thick that tend to persist laterally. Keratose sponge layers often have smooth bases and more irregular tops. Layers of mostly fine-grained detrital carbonate may locally have terminated sponge growth.

likely resulted from trapping and binding (Tosti and Riding, 2017). Reworked columns at Port au Port indicate synsedimentary lithification. In nearly all the cases observed, sponge bases are relatively smooth and sponge tops tend to be irregular. Thus, despite differences in immediately associated carbonate sediment (coarse at Port au Port vs. fine at Green Head), morphology (branched vs. domical), and age (Late Cambrian vs. Early Ordovician), in many respects the keratolite and stromatolite components are similar at the two localities.

4.4. Environment

These keratolite-stromatolite consortia formed in shallow water peritidal environments generally poor in shelly fossils (Pratt and James, 1986; Knight et al., 2008; Pruss and Knoll, 2017). Globally, the Late Cambrian-Early Ordovician was the prelude to an interval of major transition in marine biotas (Sepkoski Jr., 1981, fig. 5; Webby et al., 2004; Servais et al., 2016; Lee and Riding, 2018; Muscente et al., 2018; Stigall et al., 2019). The boundary interval was itself part of a significant peak in stromatolite development in North America (Peters et al., 2017, fig. 2), particularly along the margins of Laurentia (Aitken, 1967; Ahr, 1971; Chafetz, 1973; Campbell, 1976; Kennard and James, 1986; Knight and James, 1987; de Freitas and Mayr, 1995; Hersi et al., 2002; Miller et al., 2012). At the same time, metazoans were increasing in reefs (Fagerstrom, 1987; Wood, 1999), often in close association with microbial carbonates (Webby, 2002; Lee et al., 2015, 2019; Lee and Riding, 2018).

In the Boat Harbour Formation, ~100 m higher in the succession than our Green Head samples, Pruss and Knoll (2017) found that animal trace fossils and microbialite only rarely co-occur, supporting an antagonistic relationship, whereas skeletons of benthic invertebrates commonly co-vary positively with thrombolites, suggesting facilitation between microbial bioherms and at least some animals, which is also inferred in the “Green Head Mound Complex” (Pratt and James, 1982). In these dynamic peritidal environments, it is possible that keratosans, in consortium with stromatolites, occupied transient habitats unsuitable for other sessile metazoans. The Port au Port branched columns are arranged in broad low domes, and abundant relatively coarse sediment separates the columns (Fig. 2A). In contrast, small steep-sided domes at Green Head are surrounded by fine-grained carbonate (Fig. 3A). We infer that influx and movement of coarse sediment at Port au Port engendered and maintained branching, whereas small domes at Green Head developed relatively rapidly during intervals of slower sedimentation in less dynamic muddy environments. Irrespective of associated sediment, however, the stromatolite and keratolite fabrics in both situations are generally fine-grained. At Port au Port, sponge growth/colonization across adjacent closely spaced columns suggests a locally coordinated response to environmental and/or biotic triggers.

These interlayered sponges and mats, at Port au Port and Green Head, evidently shared similar environmental preferences and tolerances. Light could have promoted photosynthesis in both mat bacteria and sponge photo-endosymbionts, water movement would have brought food for sponges and nutrients for microbial mats, and current scour may have hindered burial by sediment. Microbial mats and sponges often tolerate fluctuations in temperature (although sponges are more sensitive to elevated temperature; Webster et al., 2008), and low oxygen levels could have favored both sponges (Mills et al., 2014) and mats (Des Marais, 1990; Gutiérrez-Preciado et al., 2018). Mats and sponges alike require stable substrates and sufficient relief to avoid over-burial by sediment. These requirements, together with ability to occupy similar environments, are typical of reef consortia in general (Riding, 2002).

5. Discussion

5.1. Keratosan sponges

Keratosa (“horny sponges”) constitute a subclass of demosponge

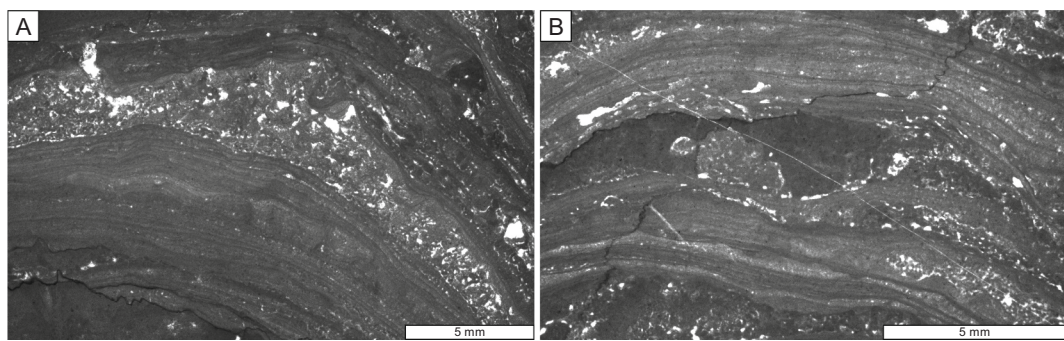


Fig. 7. Thin-section photomicrographs of domical keratolite-stromatolite; Green Head section. See positions of thin-sections in Fig. 6B. (A) Delicately laminated stromatolite overlain by keratolite with a relatively flat-base and more irregular top. (B) Intricately interlayered keratolite and stromatolite. Note isolated keratolite mass (left-center) surrounded by micrite.

(Wörheide et al., 2012). Unlike most sponges with a fossil record, keratosans do not produce either siliceous spicules (e.g., as in demosponges, hexactinellids) or heavily calcified skeletons (e.g., as in archaeocyaths, chaetetids, sphinctozoans, stromatoporoids; Wood, 1990; Reitner and Keupp, 1991). The notable exception is the hypercalcified Triassic–present day keratosan *Vaceletia* (Reitner, 1992; Reitner et al., 1997), which has superficial similarities with archaeocyaths (Wörheide, 2008; Germer et al., 2015). Instead, most keratosans are very effectively supported by a network of proteinaceous spongin fibers (Erpenbeck et al., 2012; Ehrlich et al., 2018; Jesionowski et al., 2018), as in the economically important “bath sponge”, *Spongia officinalis*. Present-day keratosans commonly contain photosynthetic symbionts, such as cyanobacteria (Wilkinson and Cheshire, 1990; Konstantinou et al., 2018), and typically occupy relatively shallow water habitats (Maldonado and Young, 1998). The absence of a rigid mineral skeleton in most keratosans hinders their present-day classification as well as their preservation and recognition as fossils. Molecular studies suggest links between Keratosa (Dictyoceratida, Dendroceratida) and a sister-group Mycospongiae (Verongida, Haliscarda, Chondrosida; Borchellini et al., 2001; Erpenbeck et al., 2012, 2020). We follow Luo and Reitner (2014) in using Keratosa in a broad sense to include all with a fibrous spongin network and lacking spicules (Minchin, 1900), since fossil material often does not preserve the additional taxonomically important features required to confidently distinguish these groups.

5.2. Synsedimentary calcification

Under suitable conditions, initially uncalcified sponges can become synsedimentarily calcified. This occurs widely in lithistid demosponges and hexactinellids, where calcification of the primary siliceous skeleton appears to be generated by microbial decomposition that ultimately preserves the sponge body as fine-grained carbonate fabrics, typically traversed by delicate tubules that represent the original supportive elements and framework (Keupp et al., 1993; Reitner, 1993; Reitner et al., 1995; Warnke, 1995). The resulting fossils have long been recognized in Phanerozoic reefs, particularly from poorly oxygenated environments (Brunton and Dixon, 1994), often in association with microbial carbonates where they create what we here term Sponge–Microbial Consortia (see Section 5.4. Terminology), as in the Cambrian–Early Ordovician (Adachi et al., 2011; Lee et al., 2016a), Mississippian (Webb, 1987; Shen and Webb, 2005; Yao et al., 2020), Late Permian–Early

Triassic (Weidlich, 2002; Brayard et al., 2011), and Mid–Late Jurassic (Leinfelder et al., 1996; Leinfelder, 2001; Aurell and Bádenas, 2015; Tomás et al., 2019).

Keratosan sponges appear to be preserved by synsedimentary calcification processes similar to those that affect siliceous sponges (Luo and Reitner, 2014): the skeletal scaffolding remains more-or-less intact, the associated soft-tissue is permineralized to CaCO₃, most likely during microbial degradation, and the skeletal network (spongin in keratosans) is either replaced or infilled by microspar (Brachert, 1991; Reitner, 1993; Reitner et al., 1995; Warnke, 1995). Nonetheless, keratosans are generally macroscopically much less conspicuous as fossils than similarly calcified siliceous sponges. This is probably due to the delicate nature of keratosan spongin network in comparison to siliceous spicules, and to the commonly less distinctive overall morphology of keratosans. Recent studies have drawn attention to keratosans in Cambrian microbial carbonates (Lee et al., 2014) and show that keratose sponges can be significant components of structures long thought to be purely microbial in origin, such as *Cryptozoon* (Lee and Riding, 2021). In significant contributions, Luo and Reitner (2014, 2016) identified “vermiform” microfabric as keratosan spongin network and demonstrated that keratosans likely have been widely overlooked in Phanerozoic shallow marine fine-grained carbonates generally (Table 1). The interlayered association with microbial carbonates characteristic of our Newfoundland examples is not unique to keratosans. Some lithistids and archaeocyaths, for example, also form relatively thin layers within and between microbial carbonate (Kruse and Reitner, 2014; Debrenne et al., 2015).

5.3. Vermiform fabric

The internal organic fibrous meshwork that supports keratose sponges (Erpenbeck et al., 2012) can be preserved in carbonates as “vermiform” fabric, a delicate microscopic sparry filamentous pattern created by the outlines of the original proteinaceous spongin network within fine-grained carbonate matrix (Luo and Reitner, 2014). Vermiform fabric is characterized by straight to slightly curved bifurcating filaments of moderately even thickness that create a somewhat irregular anastomosing network of curvilinear Y-shaped tubules (Figs. 5D, 8). In contrast, in siliceous spicular frameworks silica is deposited on proteinaceous filaments, forming regular spicules with distinctive shapes (Reiswig and Mackie, 1983; Weaver et al., 2007). For example,

Table 1

Reports of Phanerozoic fossils and fabrics regarded here as keratolite. Bold text indicates occurrences originally attributed to non-keratosan sponges. Bold underlined text indicates references in which keratosans can be discerned in illustrations but were not mentioned by the original author(s). All other occurrences were originally identified as keratosans.

Age	Locality	Lithology	Name given in paper	Reference
Middle Miocene	Spain	Deep fore-reef mud mound	Keratose sponge	Luo (2015)
Late Cretaceous (Turonian)	Spain	Between shallow-water stromatolites	Keratose sponge	Rodríguez-Martínez et al. (2012)
Early Cretaceous (late Albian)	Spain	Unknown	Keratose sponge	Luo (2015)
Late Jurassic (early Kimmeridgian)	Germany	Oyster patch reef	Keratose sponge	Luo (2015)
Middle Triassic	Germany	Crinoid reef	Keratose sponge	Luo (2015)
Middle Triassic (Ladinian)	Germany	<i>Placunopsis</i> -stromatolite reef	Keratose sponge	Luo and Reitner (2016)
Middle Triassic	Germany	<i>Placunopsis</i> reef	Keratose sponge	Luo (2015)
Middle Triassic (Anisian)	Poland	Stromatolite	Keratose sponge	Luo and Reitner (2014)
Early Triassic (Smithian)	Utah, USA	Sponge-serpulid-microbial reef	Lyssacine hexactinellids	Brayard et al. (2011, supp. fig. 2)
Early Triassic (Griesbachian)	Iran	Thrombolite	Keratose sponge	Heindel et al. (2018)
Early Triassic (Griesbachian)	Turkey	Thrombolite	Keratose sponge	Heindel et al. (2018)
Early Triassic (Griesbachian)	Armenia	Stromatolite	Keratose sponge	Friesenbichler et al. (2018)
Earliest Triassic	Hubei, China	Stromatolite	Micrite with meshlike spongy texture	Adachi et al. (2017, fig. 8D)
Earliest Triassic	Iran	Ostracod wackestone	Keratose sponge	Luo (2015)
Mississippian (Visean)	Belgium	<i>Spongistroma mæandrinum</i>	Canal system	Gürich (1906)
Mississippian (Visean)	United Kingdom	Stromatolite	Keratose sponge	Luo and Reitner (2016)
Late Devonian (Famennian)	Utah, USA	Stromatolite	Keratose sponge	Stock and Sandberg (2019)
Late Devonian (Frasnian)	Germany	Mud mound with <i>Renalcis</i> and hexactinellids	Keratose sponge	Ahlbrecht (1997), identified by Luo (2015)
Late Devonian (Frasnian)	Alberta, Canada	Stromatactis mud mound	Non-lithistid demosponge	Zhou and Pratt (2019)
Late Devonian	Belgium	Unknown	Vermiform microstructure	Pratt (1982, fig. 15A, B)
Middle Devonian (Givetian)	France	Rugose- <i>Rothpletzella</i> -sponge reef	Keratose sponge	Reitner et al. (2001); Luo and Reitner (2014)
Middle Devonian (Eifelian–Givetian)	Morocco	Holland mud mound	Keratose sponge	Luo (2015)
Late Ordovician (Katian)	Jiangxi, China	Tetradiid-sponge reef, micritic limestone, intraskeletal crypt	Siliceous sponge (Kwon et al., 2012), non-lithistid demosponge (Park et al., 2015, 2017)	Kwon et al. (2012); Park et al. (2015, 2017)
Late Ordovician (Katian)	Québec, Canada	Bryozoan reef	Microtubules of keratose sponges or fungi	Larmagnat and Neuweiler (2015)
Middle–Late Ordovician (Sandbian?)	Shaanxi, China	Bivalve-sponge-microbial reef	Siliceous sponge	Lee et al. (2016b)
Middle Ordovician (Darriwilian)	Vermont, USA	Stromatoporoid-Solenopora-tabulate-lithistid-bryozoan mound	Algal crust	Kapp (1975, fig. 3); J.-H. Lee (personal observation)
Middle Ordovician (Darriwilian)	Québec, Canada	Lithistid-bryozoan-tabulate-Solenopora bioherm	Vermiform fabric	Desrochers and James (1989, fig. 7f)
Middle Ordovician (Darriwilian)	Korea	Stromatoporoid-bryozoan reef	Siliceous sponge	Hong et al. (2018)
Middle Ordovician (Darriwilian)	Korea	Brachiopod wackestone, Stromatoporoid reef	Spiculate sponge	Park et al. (2015, fig. 8B); Hong et al. (2017)
Middle Ordovician (Darriwilian)	Tarim, China	Calathiid-demosponge reef	Keratose sponge (Shen and Neuweiler, 2018), lithistid sponge (Li et al., 2017b)	Li et al. (2017b); Shen and Neuweiler (2018)
Middle Ordovician	Nevada, USA	Meiklejohn mud mound	Meshwork of uncertain origin or pelletoid(?) texture (Ross et al., 1975); vermiform microstructure (Pratt, 1982)	Ross et al. (1975, figs. 23, 25); Pratt (1982, fig. 15C, D)
Middle Ordovician	St. Petersburg, Russia	Hekker-type mud mound	Keratose sponge	J.-H. Lee (personal observation)
Early Ordovician (Floian)	Guizhou, China	Lithistid- <i>Calathium</i> reef	Keratose sponge	Li et al. (2017a)
Early Ordovician (Tremadocian–Floian)	Hubei, China	Lithistid-microbial reef	Not recognized	Liu et al. (1997, fig. 6.1–6.3)
Early Ordovician (Tremadocian–Floian)	Anhui, China	Lithistid-microbial reef	Not recognized (Adachi et al., 2009), sponge remains (Li et al., 2015)	Adachi et al. (2009, fig. 5D); Li et al. (2015, fig. 5C)
Early Ordovician	Oklahoma, USA	Stromatolite	Clotted microstructure (vermiform)	Headd (2004)
Early Ordovician	Malaysia	Sponge-bearing thrombolites and stromatolites	Lithistid sponge	Li et al. (2019a)
Early Ordovician (Tremadocian)	Thailand	“Stromatolite” of sponge-microbial association	Probable keratose sponge	Li et al. (2019b)
Early Ordovician (Tremadocian)	Korea	Lithistid-microbial reef	Spiculate sponge	Hong et al. (2014, 2015)
Early Ordovician (Tremadocian)	Korea	Stromatolite and thrombolite	Keratose sponge	Pham and Lee (2020)
Early Ordovician (Tremadocian)	Newfoundland, Canada	Thrombolite	Vermiform fabric	Pratt (1982, fig. 13C); Pratt and James (1989b, fig. 7)
Earliest Ordovician (Tremadocian)	Newfoundland, Canada	Stromatolite	Keratose sponge	This study
Latest Cambrian (Stage 10)	Newfoundland, Canada	Stromatolite	Keratose sponge	This study
Late Cambrian (Stage 10)	Korea	Ribbon rock	Keratose sponge	Lee et al. (2018)
Late Cambrian (Stage 10)	Nevada, USA	Lithistid-microbial reef	Keratose-like sponge	Lee et al. (2019)

(continued on next page)

Table 1 (continued)

Age	Locality	Lithology	Name given in paper	Reference
Late Cambrian (Jiangshanian–Stage 10?)	New York, USA	<i>Cryptozoön proliferum</i>	Keratose sponge	Lee and Riding (2021)
Late Cambrian (Jiangshanian–Stage 10)	Utah, USA	Maceriate reef, stromatolite	Lithistid sponge	Coulson and Brand (2016)
Late Cambrian (Jiangshanian–Stage 10)	Shandong and Beijing, China	Stromatolite	Siliceous sponge	Chen et al. (2014)
Late Cambrian (Jiangshanian)	Shandong and Beijing, China	Maceriate reef	Siliceous sponge	Chen et al. (2014); Lee et al. (2014)
Late Cambrian (Paibian?)	New York, USA	Stromatolite	Keratose sponge	J.-H. Lee (personal observation)
<u>Middle–Late Cambrian</u>	<u>Amadeus Basin, Australia</u>	<u><i>Madiganites mawsoni</i></u>	<u>Vermiform fabric</u>	<u>Walter (1972); Kennard (1994)</u>
Middle Cambrian (Guzhangian)	Shandong, China	Ribbon rock	Non-lithistid demosponge	Park et al. (2015, fig. 8A)
Middle Cambrian (Guzhangian)	Inner Mongolia, China	Maceriate reef	Siliceous sponge	Lee et al. (2016c)
Middle Cambrian (Drumian)	Korea	Thrombolite-sponge boundstone	Siliceous sponge	Hong et al. (2012, 2016)
Middle Cambrian (Drumian)	Shandong, China	<i>Epiphyton</i> microbialite	Sponge-like fabric (Adachi et al., 2015), unidentified siliceous sponge (Lee et al., 2016a)	Adachi et al. (2015); Lee et al. (2016a)
<u>Early Cambrian</u>	<u>South Australia</u>	<u><i>Acaciella angepina</i></u>	<u>Algal boring</u>	<u>Preiss (1971, pl. 5b)</u>
Early Cambrian (Tommotian)	Siberia, Russia	<i>Epiphyton</i> -archaeocyath reef	Keratose sponge	Luo (2015)

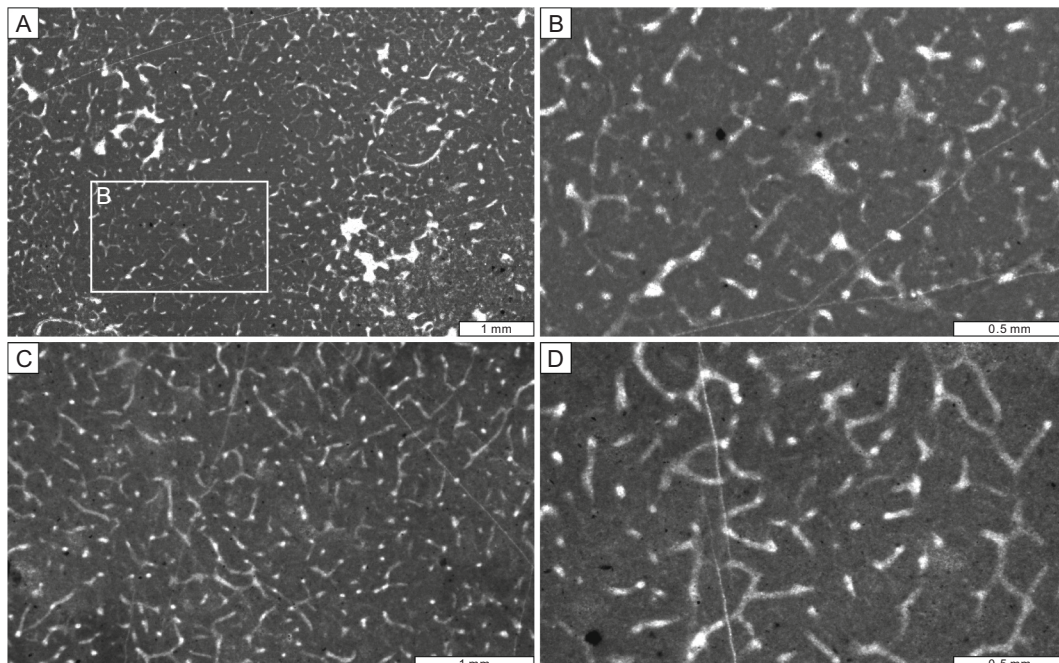


Fig. 8. Other examples of keratosan vermiciform fabric. (A, B) Middle–Late Ordovician, Shaanxi Province, China (see Lee et al., 2016b). (C, D) Late Ordovician (Katian), Jiangxi Province, China (see Park et al., 2015).

hexactinellid sponges have six-pointed spicules (hexactines) with square or rectangular cross-sections (e.g., Brachert, 1991, fig. 3A–C), whereas demosponges contain spicules of various shapes (e.g., monaxons, tetraxons), but never contain triaxons (Hooper and Van Soest, 2002).

In fossils, keratosan spongin “vermiciform” fabric has been confused with protozoans, filamentous algae, cyanobacteria and fungi. In Late Cambrian *Cryptozoön*, Hall (1883) described “numerous, minute, irregular canalici which branch and anastomose without regularity”. Gürich (1906, p. 44) described “des canaux coloniaux curvilignes et vermiciformes” (curvilinear and vermiciform colonial canals) in Mississippian *Spongostroma*, which he (p. 32) provisionally interpreted as protozoans due to their structural irregularity. Referring to *Cryptozoön*, Walter (1972) described similar fabric in Cambrian *Madiganites mawsoni*, termed it “vermiciform”, and interpreted it as the remains of algal

filaments. Bertrand-Sarfati (1976, p. 255) was uncertain of the origin of vermiciform fabric, but noted that it occurred sporadically in the late Proterozoic. Kennard (1994, p. 459) interpreted Middle to Late Cambrian vermiciform microstructure as molds of “sheaths and trichomes”. Reitner (1994, p. 405) initially compared vermiciform fabric with fungal mycelia. Subsequently, Reitner et al. (2001) suggested that vermiciform fabric represents the remains of keratose sponges, and 3-D fabric reconstruction by serial grinding tomography confirmed its morphologic similarity to the fibrous spongin network of keratose demosponges (Luo and Reitner, 2014). As comprehensively pointed out by Luo (2015), vermiciform fabric has often been mistaken for the spicular framework of siliceous sponges, including lithistids, or simply overlooked (Table 1). Late Cambrian *Cryptozoön* was long regarded as a “classic” stromatolite (Logan, 1961), even though the “canalici”

recognized in it by Hall (1883) reflect the presence of keratosan sponges (Lee and Riding, 2021).

5.4. Terminology

We propose the term keratolite for carbonate that preserves the vermiform outlines (e.g., Figs. 5D, 8) of the originally spongin keratosan skeleton. Keratolite characteristically consists of dense fine-grained millimetric to centimetric layers that represent synsedimentarily calcified organic tissue initially supported by a network of anastomosing spongin fibers. Internally, keratolite fabric can range from irregularly (Fig. 7A) to sub-millimetrically layered (Fig. 5A, B). Locally, it can incorporate fine sand grains (Lee and Riding, 2021). Keratolite can be closely associated with stromatolite (laminated microbial carbonate), as in our Newfoundland examples, as well as with diverse metazoan and other microbial reef fabrics (Table 1). In addition to vermiform fabric, cylindrical outlines and central cavities (spongocoel) typical of filter-feeding organisms can occasionally be recognized (Lee et al., 2014, fig. 7A–C).

In contrast to keratosan sponges, which have commonly been overlooked (Luo and Reitner, 2016), rock-forming associations between siliceous sponges and microbial carbonates are well-documented in the Phanerozoic (Brunton and Dixon, 1994). In Jurassic reefs, lithified siliceous sponges, typically lithistids and hexactinellids with distinctive spiculate skeletons, have variously been termed tuberoid, tuberolith (Fritz, 1958), spongolith (Geyer, 1962) and spongiolite (Keupp et al., 1993, 1996; also spelt spongolite, e.g., Gammon, 2000; Gammon et al., 2000; Gammon and James, 2003). To standardize terminology, we suggest that spongiolite should be restricted to refer to synsedimentarily calcified *siliceous* sponges. In this usage, keratolite (synsedimentarily calcified *proteinaceous* sponge) and spongiolite are varieties of synsedimentarily calcified sponge that, in close combination with microbial carbonates, create Sponge–Microbial Consortia. These likely originated in the late Proterozoic (Seilacher, 1999).

5.5. Keratolite distribution and recognition

Porifera are widely regarded as the oldest metazoan group (Feuda et al., 2017; Simon et al., 2017). The earliest currently confirmed sponge fossils are earliest Cambrian (Fortunian) in age (Chang et al., 2017, 2019), and keratosans are preserved in Early (Luo et al., 2020) and Middle Cambrian Burgess Shale-type biotas (Botting et al., 2013; Ehrlich et al., 2013; Yang et al., 2017). Although many uncertainties remain (Antcliffe et al., 2014; Botting and Muir, 2018; Nettersheim et al., 2019), biomarker (Love et al., 2009; Sperling and Stockey, 2018) and phylogenetic (Wörheide et al., 2012) studies suggest the likelihood that sponges were extant in the Neoproterozoic.

Present-day sponges harbor diverse inter- and intracellular symbiotic microbes (Rützler, 1990, 2012; Reitner, 1993; Rodriguez-Marconi et al., 2015) that can constitute a significant proportion of body mass (Hentschel et al., 2006), in some cases up to 40% (Taylor et al., 2007). These bacteria participate in key functional roles that facilitate nutrition, and provide metabolic pathways not otherwise available (Taylor et al., 2007; Richardson et al., 2012; Pita et al., 2018). Secondary metabolites can also be effective in defense (Taylor et al., 2007), and biofilms can assist sponge larval settlement (Whalan and Webster, 2014). Seafloors in the late Proterozoic are generally thought to have been poorly oxygenated and dominated by bacteria (Gingras et al., 2011; Evans et al., 2019). Bacteria and sponges likely became intimately associated as soon as sponges evolved (Li et al., 1998; Pick et al., 2010; Yin et al., 2015). Sponges, in addition to having low oxygen requirements (Mills and Canfield, 2014) and interacting intensely with microbes, can accumulate and colonize allochthonous sediment (Schönberg, 2016), similar to microbial mats. Thus, it would not be surprising if sponges, from very early in their history, were intimately associated with stromatolites and thrombolites (Seilacher, 1999; Hadfield, 2011; Antcliffe et al., 2014;

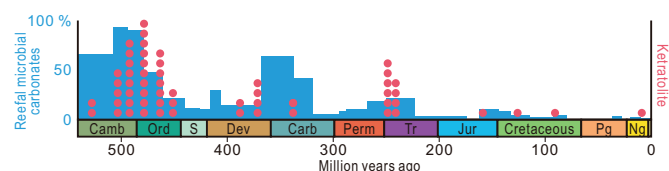


Fig. 9. Stratigraphic distribution of examples of keratolite in Phanerozoic marine limestones shown by red dots (data in Table 1) superimposed on abundance of reefal microbial carbonates (after Kiessling, 2002; Riding et al., 2019).

Droser and Gehling, 2015; Wood and Penny, 2018). Fabrics resembling keratolite occur in the late Proterozoic (Vologdin, 1962, pl. 61; Bertrand-Sarfati, 1976, p. 255; Luo, 2015, fig. 6.3).

Sponge calcification can involve microbial activity (Reitner, 1993; Reitner et al., 1995), and the conditions necessary for synsedimentary calcification to preserve keratosans were likely enhanced at times when microbial calcification in general was widespread. The secular distribution of keratolite compiled here (Table 1) broadly coincides with intervals when reefal microbial carbonates were generally abundant: Cambrian–Ordovician, Late Devonian–Mississippian, Early–Middle Triassic, and Late Jurassic–Cretaceous (Riding, 2006, fig. 6; Fig. 9). However, it is also possible that calcifying endosymbiotic bacteria might be involved in keratosan calcification, as in some present-day siliceous demosponges (Uriz et al., 2012; Garate et al., 2017).

The presence of fossil keratosans in carbonate sediment is only clearly revealed by recognition of vermiform fabric in thin-section (e.g., Lee et al., 2010, 2014; Luo and Reitner, 2014). Current understanding suggests that, despite their local volumetric abundance (Hong et al., 2016), keratosans do not create morphotypes readily distinguishable from those of stromatolites, and their overall form probably broadly reflects environmental controls. This underscores the likelihood that keratosan–microbial associations have often gone unnoticed and may have been widely mistaken as purely stromatolitic (i.e., microbial) in origin. Many putative “stromatolites” of the past 500 or more million years may harbor substantial volumes of previously unrecognized keratolite.

6. Conclusions

1. Keratolite (new term) is defined as keratosan sponge carbonate dominated by vermiform fabric that preserves the outlines of the original spongin skeleton.
2. Branched columnar and domical morphotypes formed by keratolite–stromatolite consortia in the Late Cambrian–Early Ordovician of Newfoundland are macroscopically indistinguishable from similar morphotypes that are entirely stromatolite.
3. In these deposits, keratolite is intimately interlayered with stromatolite fabric and forms layers that can be traced across domes, and from column to column in branched forms. The keratosan sponge layers typically display smooth bases and irregular tops. They constitute ~38–50% of the combined keratolite–stromatolite volume.
4. Microscopically, keratolite is distinguished by pervasive vermiform fabric. This distinctive delicate, sparry, anastomosing filamentous network results from synsedimentary calcification of the supportive keratosan spongin framework within fine-grained carbonate. In contrast, associated fine-grained stromatolites in our samples lack vermiform fabric and often display evenly layered and also cross-cutting laminae that likely resulted from agglutination of allochthonous sediment. Keratolite and stromatolite both experienced synsedimentary lithification, as shown by reworked fragments.
5. We suggest that spongiolite (originally *siliceous* sponge), and keratolite (originally *proteinaceous* sponge) are both varieties of

- synsedimentarily calcified sponge that, in close association with microbial carbonates, create Sponge–Microbial Consortia.
6. The macroscopic similarities of keratolite and stromatolite, together with the long geological range of keratosans, make it likely that keratolite has been mistaken for stromatolite throughout the Phanerozoic, and possibly in the late Proterozoic too.

Declaration of Competing Interest

The authors declare that they have no known competing financial interests or personal relationships that could have appeared to influence the work reported in this paper.

Acknowledgements

We are very grateful to two reviewers for helpful comments and suggestions that improved the final manuscript, and to Isabel Montañez for expert editorial guidance. We thank Svend Stouge for showing us localities at Isthmus Bay; K.R. Kwon and Y.J. Noh for sample preparation; and J. Park for Fig. 8C, D. Support for J.-H.L. was provided by the National Research Foundation of Korea (2019R1A2C4069278).

References

- Adachi, N., Ezaki, Y., Liu, J., Cao, J., 2009. Early Ordovician reef construction in Anhui Province, South China: A geobiological transition from microbial- to metazoan-dominant reefs. *Sediment. Geol.* 220, 1–11. <https://doi.org/10.1016/j.sedgeo.2009.05.012>.
- Adachi, N., Asada, Y., Ezaki, Y., Liu, J., 2017. Stromatolites near the Permian–Triassic boundary in Chongyang, Hubei Province, South China: A geobiological window into palaeo-oceanic fluctuations following the end-Permian extinction. *Palaeogeography, Palaeoclimatology, Palaeoecology* 475, 55–69. <https://doi.org/10.1016/j.palaeo.2017.01.030>.
- Adachi, N., Ezaki, Y., Liu, J., 2011. Early Ordovician shift in reef construction from microbial to metazoan reefs. *Palaeos* 26, 106–114. <https://doi.org/10.2110/palo.2010.p10-097r>.
- Adachi, N., Kotani, A., Ezaki, Y., Liu, J., 2015. Cambrian Series 3 lithistid sponge–microbial reefs in Shandong Province, North China: reef development after the disappearance of archaeocyathids. *Lethaia* 48, 405–416. <https://doi.org/10.1111/let.12118>.
- Ahlbrecht, J., 1997. *Verkalkte Mikrobenrelikte und kryptische Habitate des Rübeland-Mikrobialiths (Elbingeröder Riffkomplex, Harz, Mittel-Oberdevon)*. Diploma Thesis. University of Göttingen (175 pp.).
- Ahr, W.M., 1971. Paleoenvironment, algal structures, and fossil algae in the Upper Cambrian of central Texas. *J. Sediment. Petrol.* 41, 205–216. <https://doi.org/10.1306/74d72225-2b21-11d7-8648000102c1865d>.
- Atkin, J.D., 1967. Classification and environmental significance of cryptalgal limestones and dolomites, with illustrations from the Cambrian and Ordovician of southwestern Alberta. *J. Sediment. Petrol.* 37, 1163–1178. <https://doi.org/10.1306/74d7185c-2b21-11d7-8648000102c1865d>.
- Antcliffe, J.B., Callow, R.H., Brasier, M.D., 2014. Giving the early fossil record of sponges a squeeze. *Biol. Rev.* 89, 972–1004. <https://doi.org/10.1111/brv.12090>.
- Aurell, M., Bädénas, B., 2015. Facies architecture of a microbial–siliceous sponge-dominated carbonate platform: the Bajocian of Moscardón (Middle Jurassic, Spain). In: Bosence, D.W.J., Gibbons, K.A., Le Heron, D.P., Morgan, W.A., Pritchard, T., Vining, B.A. (Eds.), *Microbial Carbonates in Space and Time: Implications for Global Exploration and Production*, Geological Society of London Special Publications 418. The Geological Society of London, London, pp. 155–174. <https://doi.org/10.1144/SP418.1>.
- Bertrand-Sarfati, J., 1976. An attempt to classify Late Precambrian stromatolite microstructures. In: Walter, M.R. (Ed.), *Stromatolites. Developments in Sedimentology*, vol. 20. Elsevier, pp. 251–259. [https://doi.org/10.1016/s0070-4571\(08\)71138-5](https://doi.org/10.1016/s0070-4571(08)71138-5).
- Bertrand-Sarfati, J., Monty, C.L.V., 1994. *Phanerozoic Stromatolites II*. Kluwer Academic, Dordrecht (471 pp.).
- Black, M., 1933. The algal sedimentation of Andros Island Bahamas. *Philos. Trans. Roy. Soc. Lond. B. Biol. Sci.* 222, 165–192. <https://doi.org/10.1098/rstb.1932.0015>.
- Borchiellini, C., Manuel, M., Alivon, E., Boury-Esnault, N., Vacelet, J., Le Parco, Y., 2001. Sponge paraphyly and the origin of Metazoa. *J. Evol. Biol.* 14, 171–179. <https://doi.org/10.1046/j.1420-9101.2001.00244.x>.
- Botting, J.P., Muir, L.A., 2018. Early sponge evolution: A review and phylogenetic framework. *Palaeoworld* 27, 1–29. <https://doi.org/10.1016/j.palwor.2017.07.001>.
- Botting, J.P., Muir, L.A., Lin, J.-P., 2013. Relationships of the Cambrian Protomonaxonia (Porifera). *Palaeontol. Electron.* 16, 9A.
- Brachert, T.C., 1991. Environmental control on fossilization of siliceous sponge assemblages: a proposal. In: Reitner, J., Keupp, H. (Eds.), *Fossil and Recent Sponges*. Springer-Verlag, Berlin, Heidelberg, pp. 543–553. https://doi.org/10.1007/978-3-642-75656-6_45.
- Brayard, A., Vennin, E., Olivier, N., Bylund, K.G., Jenks, J., Stephen, D.A., Bucher, H., Hofmann, R., Goudemand, N., Escarguel, G., 2011. Transient metazoan reefs in the aftermath of the end-Permian mass extinction. *Nat. Geosci.* 4, 694–697. <https://doi.org/10.1038/ngeo1264>.
- Brunton, F.R., Dixon, O.A., 1994. Siliceous sponge-microbe biotic associations and their recurrence through the Phanerozoic as reef mound constructors. *Palaeos* 9, 370–387. <https://doi.org/10.2307/3515056>.
- Burne, R.V., Moore, L.S., 1987. Microbialites: Organosedimentary deposits of benthic microbial communities. *Palaeos* 2, 241–254. <https://doi.org/10.2307/3514674>.
- Campbell, J.A., 1976. Upper Cambrian stromatolitic biostrome, Clinetop Member of the Dotsero Formation, western Colorado. *Geol. Soc. Am. Bull.* 87, 1331–1335. [https://doi.org/10.1130/0016-7606\(1976\)87<1331:ucsbcm>2.0.co;2](https://doi.org/10.1130/0016-7606(1976)87<1331:ucsbcm>2.0.co;2).
- Chafetz, H.S., 1973. Morphological evolution of Cambrian algal mounds in response to a change in depositional environment. *J. Sediment. Petrol.* 43, 435–446. <https://doi.org/10.1306/74d7278e-2b21-11d7-8648000102c1865d>.
- Chang, S., Feng, Q., Clausen, S., Zhang, L., 2017. Sponge spicules from the lower Cambrian in the Yanjiahe Formation, South China: The earliest biomimeticizing sponge record. *Palaeogeogr. Palaeoclimatol. Palaeoecol.* 474, 36–44. <https://doi.org/10.1016/j.palaeo.2016.06.032>.
- Chang, S., Zhang, L., Clausen, S., Bottjer, D.J., Feng, Q., 2019. The Ediacaran–Cambrian rise of siliceous sponges and development of modern oceanic ecosystems. *Precambrian Res.* 333, 105438. <https://doi.org/10.1016/j.precamres.2019.105438>.
- Chen, J., Lee, J.-H., Woo, J., 2014. Formative mechanisms, depositional processes, and geological implications of Furongian (late Cambrian) reefs in the North China Platform. *Palaeogeogr. Palaeoclimatol. Palaeoecol.* 414, 246–259. <https://doi.org/10.1016/j.palaeo.2014.09.004>.
- Coulson, K.P., Brand, L.R., 2016. Lithistid sponge–microbial reef-building communities construct laminated, Upper Cambrian (Furongian) ‘stromatolites’. *Palaeos* 31, 358–370. <https://doi.org/10.2110/palo.2016.029>.
- Dawson, J.W., 1876. Notes on the Occurrence of *Eozoon canadense* at Côte St. Pierre. *Q. J. Geol. Soc. Lond.* 32, 66–75. <https://doi.org/10.1144/GSL.JGS.1876.032.01-04.10>.
- Dawson, J.W., 1896. Note on *Cryptozoon* and other ancient fossils. *The Canadian Record of Science* 7, 203–219.
- Debrenne, F., Zhuravlev, A.Y., Kruse, P.D., 2015. General features of the Archaeocyatha. In: Stearn, C.W. (Ed.), *Treatise on Invertebrate Paleontology*, Part E, Porifera, Revised, Hypercalced Porifera, vol. 4 and 5. The University of Kansas Paleontological Institute, Lawrence, Kansas, pp. 845–922.
- Des Marais, D.J., 1990. Microbial mats and the early evolution of life. *Trends Ecol. Evol.* 5, 140–144. [https://doi.org/10.1016/0169-5347\(90\)90219-4](https://doi.org/10.1016/0169-5347(90)90219-4).
- Desrochers, A., James, N.P., 1989. Middle Ordovician (Chazy) bioherms and biostromes of the Mingan Islands, Quebec. In: Geldsetzer, H.H.J., James, N.P., Tebbutt, G.E. (Eds.), *Reefs: Canada and Adjacent Areas*. Canadian Society of Petroleum Geologists Memoir, vol. 13. Canadian Society of Petroleum Geologists, pp. 183–191.
- Droser, M.L., Gehling, J.G., 2015. The advent of animals: the view from the Ediacaran. *Proc. Natl. Acad. Sci.* 112, 4865–4870. <https://doi.org/10.1073/pnas.1403669112>.
- Ehrlich, H., Rigby, J.K., Botting, J.P., Tsurkan, M.V., Werner, C., Schwille, P., Petrasek, Z., Pisera, A., Simon, P., Sivkov, V.N., Vyalikh, D.V., Molodtsov, S.L., Kurek, D., Kammer, M., Hunoldt, S., Born, R., Stawski, D., Steinholz, A., Babchenko, V.V., Geisler, T., 2013. Discovery of 505-million-year old chitin in the basal demosponge *Vauxia gracilenta*. *Sci. Rep.* 3, 3497. <https://doi.org/10.1038/srep03497>.
- Ehrlich, H., Wysokowski, M., Zoltowska-Aksamitowska, S., Petrenko, I., Jesionowski, T., 2018. Collagens of poriferan origin. *Mar. Drugs* 16, 79. <https://doi.org/10.3390/mdl6030079>.
- Elias, R.J., Lee, D.-J., Pratt, B.R., 2021. The “earliest tabulate corals” are not tabulates. *Geology* 49, 304–308. <https://doi.org/10.1130/g48235.1>.
- Erpenbeck, D., Sutcliffe, P., Cook Sde, C., Dietzel, A., Maldonado, M., van Soest, R.W., Hooper, J.N., Wörheide, G., 2012. Horny sponges and their affairs: on the phylogenetic relationships of keratose sponges. *Mol. Phylogenet. Evol.* 63, 809–816. <https://doi.org/10.1016/j.ympev.2012.02.024>.
- Erpenbeck, D., Galitz, A., Ekins, M., Cook, S.d.C., Soest, R.W.M., Hooper, J.N.A., Wörheide, G., 2020. Soft sponges with tricky tree: on the phylogeny of dictyoceratid sponges. *J. Zool. Syst. Evol. Res.* 58, 27–40. <https://doi.org/10.1111/jzs.12351>.
- Evans, S.D., Gehling, J.G., Droser, M.L., 2019. Slime travelers: early evidence of animal mobility and feeding in an organic mat world. *Geobiology* 17, 490–509. <https://doi.org/10.1111/gbi.12351>.
- Fagerstrom, J.A., 1987. *The Evolution of Reef Communities*. John Wiley and Sons, New York (600 pp.).
- Feuda, R., Dohrmann, M., Pett, W., Philippe, H., Rota-Stabelli, O., Lartillot, N., Wörheide, G., Pisani, D., 2017. Improved modeling of compositional heterogeneity supports sponges as sister to all other animals. *Curr. Biol.* 27, 3864–3870. <https://doi.org/10.1016/j.cub.2017.11.008>.
- Flügel, E., Reinhardt, J., 1989. Uppermost Permian reefs in Skyros (Greece) and Sichuan (China): implications for the Late Permian extinction event. *Palaeos* 4, 502–518. <https://doi.org/10.2307/3514742>.
- de Freitas, T., Mayr, U., 1995. Kilometre-scale microbial buildups in a rimmed carbonate platform succession, Arctic Canada: new insight on Lower Ordovician reef facies. *Bull. Can. Petrol. Geol.* 43, 407–432. <https://doi.org/10.35767/gscpgbull.43.4.407>.
- Friesenbichler, E., Richoz, S., Baud, A., Krystyn, L., Sahakyan, L., Vardanyan, S., Peckmann, J., Reitner, J., Heindel, K., 2018. Sponge–microbial build-ups from the lowermost Triassic Chanakhchi section in southern Armenia: Microfacies and stable carbon isotopes. *Palaeogeogr. Palaeoclimatol. Palaeoecol.* 490, 653–672. <https://doi.org/10.1016/j.palaeo.2017.11.056>.
- Fritz, G.K., 1958. Schwammstözen, Tuberkolith und Schuttbreccien im Weißen Jura der Schwäbischen Alb: Eine vergleichende petrogenetische Untersuchung, vol. 13.

- Arbeiten Geologisch Paläontologisches Institut Technische Hochschule (Neue Folge), Stuttgart (118 pp). (in German).
- Gammon, P.R., 2000. Spiculites and spongolites. In: Middleton, G.V. (Ed.), Encyclopedia of Sediments and Sedimentary Rocks. Springer, pp. 681–683.
- Gammon, P.R., James, N.P., 2003. Paleoenvironmental controls on upper eocene biosiliceous neritic sediments, southern Australia. *J. Sediment. Res.* 73, 957–972. <https://doi.org/10.1306/032103730957>.
- Gammon, P.R., James, N.P., Pisera, A., 2000. Eocene spiculites and spongolites in southwestern Australia: not deep, not polar, but shallow and warm. *Geology* 28, 855–858. [https://doi.org/10.1130/0091-7613\(2000\)28<855:ESASIS>2.0.CO;2](https://doi.org/10.1130/0091-7613(2000)28<855:ESASIS>2.0.CO;2).
- Garate, L., Sureda, J., Agell, G., Uriz, M.J., 2017. Endosymbiotic calcifying bacteria across sponge species and oceans. *Sci. Rep.* 7, 43674. <https://doi.org/10.1038/srep43674>.
- Germer, J., Mann, K., Wörheide, G., Jackson, D.J., 2015. The skeleton forming proteome of an early branching metazoan: a molecular survey of the biomineralization components employed by the coralline sponge *Vaceletia* sp. *PLoS One* 10, e0140100. <https://doi.org/10.1371/journal.pone.0140100>.
- Geyer, O.F., 1962. In: Geyer, O.F. (Ed.), Über Schwammgesteine (Spongolith, Tuberolith, Spiculit und Gaizit). Hermann-Aldinger-Festschrift, Stuttgart, pp. 51–59 (in German).
- Gingras, M., Hagadorn, J.W., Seilacher, A., Lalonde, S.V., Pecoits, E., Petrush, D., Konhauser, K.O., 2011. Possible evolution of mobile animals in association with microbial mats. *Nat. Geosci.* 4, 372–375. <https://doi.org/10.1038/ngeo1142>.
- Google, 2020. Google Maps <http://maps.google.com/>. Checked May 2020.
- Grey, K., Awramik, S.M., 2020. Handbook for the study and description of microbialites. In: Geological Survey of Western Australia Bulletin, vol. 147 (278 pp).
- Grey, K., Blake, D.H., 1999. Neoproterozoic (Cryogenian) stromatolites from the Wolfe Basin, east Kimberley, Western Australia: correlation with the Centralian Superbasin. *Aust. J. Earth Sci.* 46, 329–341. <https://doi.org/10.1046/j.1440-0952.1999.00707.x>.
- Gürich, G., 1906. Les spongiostromides du Viséen de la Province de Namur. In: Musée royal d'histoire naturelle de Belgique, Mémoires, vol. 3, pp. 1–55 (in French).
- Gutiérrez-Preciado, A., Saghai, A., Moreira, D., Zivanovic, Y., Deschamps, P., López-García, P., 2018. Functional shifts in microbial mats recapitulate early Earth metabolic transitions. *Nat. Ecol. Evol.* 2, 1700–1708. <https://doi.org/10.1038/s41559-018-0683-3>.
- Hadfield, M.G., 2011. Biofilms and marine invertebrate larvae: what bacteria produce that larvae use to choose settlement sites. *Ann. Rev. Mar. Sci.* 3, 453–470. <https://doi.org/10.1146/annurev-marine-120709-142753>.
- Hall, J., 1883. *Cryptozoon*, n.g.; *Cryptozoon proliferum*, n.sp., New York State Museum of Natural History. 36th Annual Report of the Trustees.
- Hartman, W.D., Wendt, J.W., Wiedenmayer, F., 1980. Living and fossil sponges (Notes for a short course). In: *Sedimentia*, vol. 8. University of, Miami (274 pp).
- Headd, B.J., 2004. Microstructural analysis of the Lower Ordovician Cool Creek Formation stromatolites, Arbuckle Mountains, Southern Oklahoma. M.S. Thesis. Texas Tech University (274 pp).
- Heindel, K., Foster, W.J., Richoz, S., Birgel, D., Roden, V.J., Baud, A., Brandner, R., Krystyn, L., Mohtat, T., Koşun, E., Twitchett, R.J., Reitner, J., Peckmann, J., 2018. The formation of microbial-metazoan bioherms and biostromes following the latest Permian mass extinction. *Gondwana Res.* 61, 187–202. <https://doi.org/10.1016/j.gr.2018.05.007>.
- Hentschel, U., Usher, K.M., Taylor, M.W., 2006. Marine sponges as microbial fermenters. *FEMS Microbiol. Ecol.* 55, 167–177. <https://doi.org/10.1111/j.1574-6941.2005.00046.x>.
- Hersi, O.S., Lavoie, D., Nowlan, G.S., 2002. Stratigraphy and sedimentology of the Upper Cambrian Strites Pond Formation, Philipsburg Group, southern Quebec, and implications for the Cambrian platform in eastern Canada. *Bull. Can. Petrol. Geol.* 50, 542–565.
- Hong, J., Cho, S.-H., Choh, S.-J., Woo, J., Lee, D.-J., 2012. Middle Cambrian siliceous sponge-calcimicrobe buildups (Daegi Formation, Korea): Metazoan buildup constituents in the aftermath of the Early Cambrian extinction event. *Sediment. Geol.* 253–254, 47–57. <https://doi.org/10.1016/j.sedgeo.2012.01.011>.
- Hong, J., Choh, S.-J., Lee, D.-J., 2014. Tales from the crypt: early adaptation of cryptobiotic sessile metazoans. *Palaios* 29, 95–100. <https://doi.org/10.2110/palo.2014.076>.
- Hong, J., Choh, S.-J., Lee, D.-J., 2015. Untangling intricate microbial-sponge frameworks: the contributions of sponges to Early Ordovician reefs. *Sediment. Geol.* 318, 75–84. <https://doi.org/10.1016/j.sedgeo.2015.01.003>.
- Hong, J., Lee, J.-H., Choh, S.-J., Lee, D.-J., 2016. Cambrian Series 3 carbonate platform of Korea dominated by microbial-sponge reefs. *Sediment. Geol.* 341, 58–69. <https://doi.org/10.1016/j.sedgeo.2016.04.012>.
- Hong, J., Choh, S.-J., Park, J., Lee, D.-J., 2017. Construction of the earliest stromatoporoid framework: Labechiid reefs from the Middle Ordovician of Korea. *Palaeogeogr. Palaeoclimatol. Palaeoecol.* 470, 54–62. <https://doi.org/10.1016/j.palaeo.2017.01.017>.
- Hong, J., Oh, J.-R., Lee, J.-H., Choh, S.-J., Lee, D.-J., 2018. The earliest evolutionary link of metazoan bioconstruction: Laminar stromatoporoid-bryozoan reefs from the Middle Ordovician of Korea. *Palaeogeogr. Palaeoclimatol. Palaeoecol.* 492, 126–133. <https://doi.org/10.1016/j.palaeo.2017.12.018>.
- Hooper, J.N.A., Van Soest, R.W.M., 2002. Class Demospongiae Sollas, 1885. In: Hooper, J.N.A., Van Soest, R.W.M. (Eds.), *Systema Porifera: A Guide to the Classification of Sponges*. Kluwer Academic/Plenum Publishers, New York, pp. 15–51.
- James, N.P., Stevens, R.K., Barnes, C.R., Knight, I., 1989. Evolution of a Lower Paleozoic continental-margin carbonate platform, northern Canadian Appalachians. In:
- Crevello, P.D., Wilson, J.L., Sarg, J.F., Read, J.F. (Eds.), *Controls on Carbonate Platform and Basin Development*. SEPM Special Publication 44. SEPM, pp. 123–146.
- Jesionowski, T., Norman, M., Zoltowska-Aksamitowska, S., Petrenko, I., Joseph, Y., Ehrlich, H., 2018. Marine spongin: naturally prefabricated 3D scaffold-based biomaterial. *Mar. Drugs* 16, 88. <https://doi.org/10.3390/md16030088>.
- Ji, Z., Barnes, C.R., 1994. Conodont paleoecology of the Lower Ordovician St. George Group, Port au Port Peninsula, western Newfoundland. *J. Paleontol.* 1368–1383. <https://doi.org/10.1017/S00223360003434X>.
- Kalkowsky, E., 1908. Oolith und Stromatolith im nordeutschen Buntsandstein. *Z. Dtsch. Geol. Ges.* 60, 68–125 (in German).
- Kapp, U.S., 1975. Paleoecology of Middle Ordovician stromatoporoid mounds in Vermont. *Lethaia* 8, 195–207. <https://doi.org/10.1111/j.1502-3931.1975.tb00923.x>.
- Kennard, J.M., 1994. Thrombolites and stromatolites within shale-carbonate cycles, Middle-Late Cambrian Shannon Formation, Amadeus Basin, central Australia. In: Bertrand-Sarfati, J., Monty, C.L.V. (Eds.), *Phanerozoic Stromatolites II*. Kluwer Academic, Netherlands, pp. 443–471.
- Kennard, J.M., James, N.P., 1986. Thrombolites and stromatolites: two distinct types of microbial structures. *Palaios* 1, 492–503. <https://doi.org/10.2307/3514631>.
- Kennard, J.M., Chow, N., James, N.P., 1989. Thrombolite-stromatolite bioherm, Middle Cambrian, Port au Port Peninsula, western Newfoundland. In: Geldzetter, H.H.J., James, N.P., Tebbutt, G.E. (Eds.), *Reefs: Canada and Adjacent Areas*. Canadian Society of Petroleum Geologists Memoir, vol. 13. Canadian Society of Petroleum Geologists, pp. 151–155.
- Keupp, H., Jenisch, A., Herrmann, R., Neuweiler, F., Reitner, J., 1993. Microbial carbonate crusts - a key to the environmental analysis of fossil spongiosites? *Facies* 29, 41–54. <https://doi.org/10.1007/BF02536916>.
- Keupp, H., Brugger, H., Galling, U., Hefta, J., Herrmann, R., Jenisch, A., Kempe, S., Michaelis, W., Seifert, R., Thiel, V., 1996. Paleobiological controls of Jurassic spongiosites. In: Reitner, J., Neuweiler, F., Gunkel, F. (Eds.), *Global and Regional Controls on Biogenic Sedimentation. I. Reef Evolution*. Göttinger Arbeiten zur Geologie und Paläontologie Sonderband 2, Göttingen, pp. 209–214.
- Kiessling, W., 2002. Secular variations in the Phanerozoic reef ecosystem. In: Kiessling, W., Flügel, E., Golonka, J. (Eds.), *Phanerozoic Reef Patterns*. SEPM Special Publication 72. SEPM, Tulsa, pp. 625–690. <https://doi.org/10.2110/pec.02.72.0625>.
- Knight, I., James, N.P., 1987. The stratigraphy of the Lower Ordovician St. George Group, western Newfoundland: the interaction between eustasy and tectonics. *Can. J. Earth Sci.* 24, 1927–1951. <https://doi.org/10.1139/e87-185>.
- Knight, I., Azmy, K., Boyce, W.D., Lavoie, D., 2008. Tremadocian carbonate rocks of the lower St. George Group, Port au Port Peninsula, western Newfoundland: lithostratigraphic setting of diagenetic, isotopic and geochemistry studies. In: Geological Survey Report 08-1, Current Research. Newfoundland and Labrador Department of Natural Resources, pp. 115–149.
- Konhauser, K.O., 2006. Introduction to Geomicrobiology. Wiley-Blackwell (440 pp).
- Konstantinou, D., Gerovasiliou, V., Voultsiadou, E., Gkelis, S., 2018. Sponges-Cyanobacteria associations: Global diversity overview and new data from the Eastern Mediterranean. *PLoS One* 13, e0195001. <https://doi.org/10.1371/journal.pone.0195001>.
- Kruse, P.D., Reitner, J.R., 2014. Northern Australian microbial-metazoan reefs after the mid-Cambrian mass extinction. In: *Memoirs of the Association of Australasian Palaeontologists*, vol. 45, pp. 31–53.
- Kwon, S.-W., Park, J., Choh, S.-J., Lee, D.-J., 2012. Tetradiid-siliceous sponge patch reefs from the Xiazen Formation (late Katian), southeast China: A new Late Ordovician reef association. *Sediment. Geol.* 267–268, 15–24. <https://doi.org/10.1016/j.sedgeo.2012.04.001>.
- Larmagnat, S., Neuweiler, F., 2015. Taphonomic filtering in Ordovician bryozoan carbonate mounds, Trenton Group, Montmorency Falls, Quebec, Canada. *Palaios* 30, 169–180. <https://doi.org/10.2110/palo.2013.120>.
- Lavoie, D., 2019. The Cambrian-Devonian Laurentian platforms and foreland basins in eastern Canada. In: Miall, A.D. (Ed.), *The Sedimentary Basins of the United States and Canada*. Elsevier, second edition, pp. 77–128. <https://doi.org/10.1016/b978-0-444-63895-3.00003-6>.
- Lavoie, D., Desrochers, A., Dix, G., Knight, I., Hersi, O.S., 2012. The Great American Carbonate Bank in Eastern Canada: an overview. In: Derby, J.R., Fritz, R.D., Longacre, S.A., Morgan, W.A., Sternbach, C.A. (Eds.), *The Great American Carbonate Bank: The Geology and Economic Resources of the Cambrian-Ordovician Sank Megasequence of Laurentia*. AAPG Memoir 98. AAPG, pp. 499–523. <https://doi.org/10.1306/13331504M983503>.
- Lee, J.-H., Riding, R., 2018. Marine oxygenation, lithistid sponges, and the early history of Paleozoic skeletal reefs. *Earth Sci. Rev.* 181, 98–121. <https://doi.org/10.1016/j.earscirev.2018.04.003>.
- Lee, J.-H., Riding, R., 2021. The ‘classic stromatolite’ *Cryptozoon* is a keratose sponge-microbial consortium. *Geobiology* 19, 189–198. <https://doi.org/10.1111/gbi.12422>.
- Lee, J.-H., Chen, J., Chough, S.K., 2010. Paleoenvironmental implications of an extensive macerite microbial bed in the Furongian Chaomidian Formation, Shandong Province, China. *Palaeogeogr. Palaeoclimatol. Palaeoecol.* 297, 621–632. <https://doi.org/10.1016/j.palaeo.2010.09.012>.
- Lee, J.-H., Chen, J., Choh, S.-J., Lee, D.-J., Han, Z., Chough, S.K., 2014. Furongian (late Cambrian) sponge-microbial maze-like reefs in the North China Platform. *Palaios* 29, 27–37. <https://doi.org/10.2110/palo.2013.050>.
- Lee, J.-H., Chen, J., Chough, S.K., 2015. The middle-late Cambrian reef transition and related geological events: a review and new view. *Earth Sci. Rev.* 145, 66–84. <https://doi.org/10.1016/j.earscirev.2015.03.002>.

- Lee, J.-H., Hong, J., Choh, S.-J., Lee, D.-J., Woo, J., Riding, R., 2016a. Early recovery of sponge framework reefs after Cambrian archaeocyath extinction: Zhangxian Formation (early Cambrian Series 3), Shandong, North China. *Palaeogeogr. Palaeoclimatol. Palaeoecol.* 457, 269–276. <https://doi.org/10.1016/j.palaeo.2016.06.018>.
- Lee, J.-H., Hong, J., Lee, D.-J., Choh, S.-J., 2016b. A new Middle Ordovician bivalve–siliceous sponge–microbe reef-building consortium from North China. *Palaeogeogr. Palaeoclimatol. Palaeoecol.* 457, 23–30. <https://doi.org/10.1016/j.palaeo.2016.05.034>.
- Lee, J.-H., Kim, B.-J., Liang, K., Park, T.-Y., Choh, S.-J., Lee, D.-J., Woo, J., 2016c. Cambrian reefs in the western North China Platform, Wuhan, Inner Mongolia. *Acta Geol. Sin.* 90, 1946–1954. <https://doi.org/10.1111/1755-6724.1301410.1111/1755-6724.13014>.
- Lee, J.-H., Choh, S.-J., Lee, D.-J., 2018. Limestone-Shale Couplet Revisited: Upper Cambrian (Furongian) Hwajeon Formation, Taebaeksan Basin, Korea. Geological Society of America Abstracts with Programs 50. <https://doi.org/10.1130/abs/2018AM-317117>.
- Lee, J.-H., Dattilo, B.F., Mrozek, S., Miller, J.F., Riding, R., 2019. Lithistid sponge-microbial reefs, Nevada, USA: Filling the late Cambrian ‘reef gap’. *Palaeogeogr. Palaeoclimatol. Palaeoecol.* 520, 251–262. <https://doi.org/10.1016/j.palaeo.2019.02.003>.
- Leinfelder, R.R., 2001. Jurassic reef ecosystems. In: Stanley, G.D. (Ed.), *The History and Sedimentology of Ancient Reef Systems*. Kluwer Academic/Plenum Publishers, New York, pp. 251–309. https://doi.org/10.1007/978-1-4615-1219-6_8.
- Leinfelder, R.R., Werner, W., Nose, M., Schmid, D.U., Krautter, M., Laternser, R., Takacs, M., Hartmann, D., 1996. Paleoecology, growth parameters and dynamics of coral, sponge and microbialite reefs from the late Jurassic. In: Reitner, J., Neuweiler, F., Gunkel, F. (Eds.), *Global and Regional Controls on Biogenic Sedimentation. 1. Reef Evolution. Research Reports*. Göttinger Arbeiten zur Geologie und Paläontologie, Sonderband 2, Göttingen, pp. 227–248.
- Li, C.-W., Chen, J.-Y., Hua, T.-E., 1998. Precambrian sponges with cellular structures. *Science* 279, 879–882. <https://doi.org/10.1126/science.279.5352.879>.
- Li, Q., Li, Y., Wang, J., Kiessling, W., 2015. Early Ordovician lithistid sponge–*Calathium* reefs on the Yangtze Platform and their paleoceanographic implications. *Palaeogeogr. Palaeoclimatol. Palaeoecol.* 425, 84–96. <https://doi.org/10.1016/j.palaeo.2015.02.034>.
- Li, Q., Li, Y., Kiessling, W., 2017a. The oldest labechiid stromatoporoids from intraskeletal crypts in lithistid sponge–*Calathium* reefs. *Lethaia* 50, 140–148. <https://doi.org/10.1111/let.12182>.
- Li, Q., Li, Y., Munnecke, A., 2017b. Dissecting *Calathium*-microbial frameworks: The significance of calathids for the Middle Ordovician reefs in the Tarim Basin, northwestern China. *Palaeogeogr. Palaeoclimatol. Palaeoecol.* 474, 66–78. <https://doi.org/10.1016/j.palaeo.2016.08.005>.
- Li, Q.J., Agematsu, S., Na, L., Sardsud, A.A., 2019b. Stromatolite abundance anomaly in Early Ordovician: the rise of sponge-microbial association? In: Obut, O.T., Sennikov, N.V., Kipriyanova, T.P. (Eds.), *13th International Symposium on the Ordovician System, Novosibirsk*, pp. 113–114.
- Li, Q.-J., Sone, M., Lehnert, O., Na, L., 2019a. Early Ordovician sponge-bearing microbialites from Peninsular Malaysia: The initial rise of metazoans in reefs. *Palaeoworld* 28, 80–95. <https://doi.org/10.1016/j.palwor.2018.08.005>.
- Li, B., Rigby, J.K., Jiang, Y., Zhu, Z., 1997. Lower Ordovician lithistid sponges from the eastern Yangtze Gorge Area, Hubei, China. *J. Paleontol.* 71, 194–207. <https://doi.org/10.1017/S0022336000039135>.
- Logan, B.W., 1961. *Cryptozoon* and associate stromatolites from the Recent, Shark Bay, Western Australia. *J. Geol.* 69, 517–533. <https://doi.org/10.1086/626769>.
- Logan, B.W., Rezak, R., Ginsburg, R.N., 1964. Classification and environmental significance of algal stromatolites. *J. Geol.* 72, 68–83. <https://doi.org/10.1086/626965>.
- Love, G.D., Grosjean, E., Stalvies, C., File, D.A., Grotzinger, J.P., Bradley, A.S., Kelly, A.E., Bhatia, M., Meredith, W., Snape, C.E., Bowring, S.A., Condon, D.J., Summons, R.E., 2009. Fossil steroids record the appearance of Demospiongidae during the Cryogenian period. *Nature* 457, 718–721. <https://doi.org/10.1038/nature07673>.
- Luo, C., 2015. “Keratose” Sponge Fossils and Microbialites: A Geobiological Contribution to the Understanding of Metazoan Origin. Ph.D Thesis. Georg-August-Universität Göttingen (151 pp.).
- Luo, C., Reitner, J., 2014. First report of fossil “keratose” demosponges in Phanerozoic carbonates: Preservation and 3-D reconstruction. *Naturwissenschaften* 101, 467–477. <https://doi.org/10.1007/s00114-014-1176-0>.
- Luo, C., Reitner, J., 2016. ‘Stromatolites’ built by sponges and microbes - a new type of Phanerozoic bioconstruction. *Lethaia* 49, 555–570. <https://doi.org/10.1111/let.12166>.
- Luo, C., Zhao, F., Zeng, H., 2020. The first report of a vauxiid sponge from the Cambrian Chengjiang Biota. *J. Paleontol.* 94, 28–33. <https://doi.org/10.1017/jpa.2019.52>.
- Maldonado, M., Young, C.M., 1998. Limits on the bathymetric distribution of keratose sponges: a field test in deep water. *Mar. Ecol. Prog. Ser.* 174, 123–139. <https://doi.org/10.3354/meps174123>.
- Miller, J.F., Evans, K.R., Dattilo, B.F., 2012. The Great American Carbonate Bank in the miogeocline of western central Utah: tectonic influences on sedimentation. In: Derby, J.R., Fritz, R.D., Longacre, S.A., Morgan, W.A., Sternbach, C.A. (Eds.), *The Great American Carbonate Bank: The Geology and Economic Resources of the Cambrian-Ordovician Sauk Megasequence of Laurentia*, AAPG Memoir 98. AAPG, pp. 769–854. <https://doi.org/10.1306/13331516M983498>.
- Mills, D.B., Canfield, D.E., 2014. Oxygen and animal evolution: did a rise of atmospheric oxygen ‘trigger’ the origin of animals? *Bioessays* 36, 1145–1155. <https://doi.org/10.1002/bies.201400101>.
- Mills, D.B., Ward, L.M., Jones, C., Sweeten, B., Forth, M., Treusch, A.H., Canfield, D.E., 2014. Oxygen requirements of the earliest animals. *Proc. Natl. Acad. Sci.* 111, 4168–4172. <https://doi.org/10.1073/pnas.1400547111>.
- Minchin, E.A., 1900. Chapter III. Sponges. In: Lankester, E.R. (Ed.), *A Treatise on Zoology. Part II. The Porifera and Coelenterata*. A&C Black, London, pp. 1–178.
- Monty, C., 1981. *Phanerozoic Stromatolites*. Springer-Verlag, Berlin Heidelberg. <https://doi.org/10.1007/978-3-642-67913-1>.
- Muscente, A.D., Prabhu, A., Zhong, H., Eleigh, A., Meyer, M.B., Fox, P., Hazen, R.M., Knoll, A.H., 2018. Quantifying ecological impacts of mass extinctions with network analysis of fossil communities. *Proc. Natl. Acad. Sci.* 115, 5217–5222. <https://doi.org/10.1073/pnas.1711997115>.
- Nettersheim, B.J., Brocks, J.J., Schwelm, A., Hope, J.M., Not, F., Lomas, M., Schmidt, C., Schieber, R., Nowack, E.C.M., De Deckker, P., Pawłowski, J., Bowser, S.S., Bobrovskiy, I., Zonneveld, K., Kucera, M., Stuhr, M., Hallmann, C., 2019. Putative sponge biomarkers in unicellular Rhizaria question an early rise of animals. *Nat. Ecol. Evol.* 3, 577–581. <https://doi.org/10.1038/s41559-019-0806-5>.
- Noffke, N., Awramik, S.M., 2013. Stromatolites and MISS—differences between relatives. *GSA Today* 23, 4–9. <https://doi.org/10.1130/gsatg187a.1>.
- Park, J., Lee, J.-H., Hong, J., Choh, S.-J., Lee, D.-C., Lee, D.-J., 2015. An Upper Ordovician sponge-bearing micritic limestone and implication for early Palaeozoic carbonate successions. *Sediment. Geol.* 319, 124–133. <https://doi.org/10.1016/j.sedgeo.2015.02.002>.
- Park, J., Lee, J.-H., Hong, J., Choh, S.-J., Lee, D.-C., Lee, D.-J., 2017. Crouching shells, hidden sponges: unusual Late Ordovician cavities containing sponges. *Sediment. Geol.* 347, 1–9. <https://doi.org/10.1016/j.sedgeo.2016.11.003>.
- Peters, S.E., Husson, J.M., Wilcots, J., 2017. The rise and fall of stromatolites in shallow marine environments. *Geology* 45, 487–490. <https://doi.org/10.1130/g38931.1>.
- Pham, D., Lee, J.-H., 2020. Keratose sponge–microbial carbonate consortium in the columnar “stromatolites” and “thrombolite” mounds from the Lower Ordovician Mungol Formation, Yeongwol, Korea. In: Rasmussen, C.M.Ø., Stigall, A.L., Nielsen, A.T., Stouge, S., Schovsbo, N.H. (Eds.), *Zooming in on the GOBE: 2020 Virtual Annual Meeting of IGCP653. Geological Survey of Denmark and Greenland*, p. 37.
- Pick, K.S., Philippe, H., Schreiber, F., Erpenbeck, D., Jackson, D.J., Wrede, P., Wiens, M., Alie, A., Morgenstern, B., Manuel, M., Wörheide, G., 2010. Improved phylogenomic taxon sampling noticeably affects nonbilaterian relationships. *Mol. Biol. Evol.* 27, 1983–1987. <https://doi.org/10.1093/molbev/msq089>.
- Pita, L., Rix, L., Slaby, B.M., Franke, A., Hentschel, U., 2018. The sponge holobiont in a changing ocean: from microbes to ecosystems. *Microbiome* 6, 46. <https://doi.org/10.1186/s40168-018-0428-1>.
- Pratt, B.R., 1982. Stromatolitic framework of carbonate mud-mounds. *J. Sediment. Petrol.* 52, 1203–1227. <https://doi.org/10.1306/212F80FD-2B24-11D7-8648000102C1865D>.
- Pratt, B.R., James, N.P., 1982. Cryptalgal-metazoan bioherms of early Ordovician age in the St George Group, western Newfoundland. *Sedimentology* 29, 543–569. <https://doi.org/10.1111/j.1365-3091.1982.tb01733.x>.
- Pratt, B.R., James, N.P., 1986. The St George Group (Lower Ordovician) of western Newfoundland; tidal flat island model for carbonate sedimentation in shallow epeiric seas. *Sedimentology* 33, 313–343. <https://doi.org/10.1111/j.1365-3091.1986.tb00540.x>.
- Pratt, B.R., James, N.P., 1989a. Coral–Renalcis–thrombolite reef complex of Early Ordovician Age, St. George Group, western Newfoundland. In: Geldsetzer, H.H.J., James, N.P., Tebbutt, G.E. (Eds.), *Reefs: Canada and Adjacent Areas, Canadian Society of Petroleum Geologists Memoir 13*. Canadian Society of Petroleum Geologists, pp. 224–230.
- Pratt, B.R., James, N.P., 1989b. Early Ordovician thrombolite reefs, St. George Group, western Newfoundland. In: Geldsetzer, H.H.J., James, N.P., Tebbutt, G.E. (Eds.), *Reefs: Canada and Adjacent Areas, Canadian Society of Petroleum Geologists Memoir 13*. Canadian Society of Petroleum Geologists, St. John’s, pp. 231–240.
- Preiss, W.V., 1971. The Biostratigraphy and Palaeoecology of South Australian Precambrian Stromatolites. Ph.D. Thesis. University of Adelaide, Adelaide (347 pp.).
- Pruss, S.B., Knoll, A.H., 2017. Environmental covariation of metazoans and microbialites in the Lower Ordovician Boat Harbour Formation, Newfoundland. *Palaeogeogr. Palaeoclimatol. Palaeoecol.* 485, 917–929. <https://doi.org/10.1016/j.palaeo.2017.08.007>.
- Reiswig, H.M., 2002. Class Hexactinellida Schmidt, 1870. In: Hooper, J.N.A., Van Soest, R.W.M. (Eds.), *Systema Porifera: A Guide to the Classification of Sponges*. Kluwer Academic/Plenum Publishers, New York, pp. 1201–1210.
- Reiswig, H.M., Mackie, G.O., 1983. Studies on hexactinellid sponges. III. The taxonomic status of hexactinellida within the porifera. *Philos. Trans. R. Soc. Lond. Ser. B Biol. Sci.* 301, 419–428. <https://doi.org/10.1098/rstb.1983.0030>.
- Reitner, J., 1992. *Coralline Sponges: Der Versuch einer Phylogenetisch Taxonomischen Analyse*. Berliner Geowissenschaftliche Abhandlungen Reihe E, Palaeobiologie 1 (352 pp.). (in German).
- Reitner, J., 1993. Modern cryptic microbialite/metazoan facies from Lizard Island (Great Barrier Reef, Australia) formation and concepts. *Facies* 29, 3–40. <https://doi.org/10.1007/BF02536915>.
- Reitner, J., 1994. Mikrobialith-porifera fazies eines exogren/korallen patchreets des oberen korallenooliths im Steinbruch Langenberg bei Oker (Niedersachsen). Berliner geowissenschaftliche Abhandlungen E13 397–417. <https://doi.org/10.23689/fidgeo-772> (in German with English abstract).
- Reitner, J., Keupp, H., 1991. *Fossil and Recent Sponges*. Springer-Verlag, Berlin Heidelberg. <https://doi.org/10.1007/978-3-642-75656-6> (595 pp.).
- Reitner, J., Neuweller, F., Flajsz, G., Vigenar, M., Keupp, H., Meischner, D., Neuweller, F., Paul, J., Reitner, J., Warnke, K., Weller, H., Dingle, P., Hensen, C., Schäfer, P., Gautret, P., Leinfelder, R., Hüssner, H., Kaufmann, B., 1995. Mud mounds: a

- polygenetic spectrum of fine-grained carbonate buildups. *Facies* 32, 1–69. <https://doi.org/10.1007/BF02536864>.
- Reitner, J., Wörheide, G., Lange, R., Thiel, V., 1997. Biomineralization of calcified skeletons in three Pacific coralline demosponges - an approach to the evolution of basal skeletons. *Courier Forschungsinstitut Senckenberg* 201, 371–383.
- Reitner, J., Hühne, C., Thiel, V., 2001. Porifera-rich mud mounds and microbialites as indicators of environmental changes within the Devonian/Lower Carboniferous critical interval. *Terra Nostra* 4, 60–65.
- Reitner, J., Quéric, N.-V., Arp, G., 2011. Advances in Stromatolite Geobiology. In: Lecture Notes in Earth Sciences, vol. 131. Springer-Verlag, Berlin Heidelberg. <https://doi.org/10.1007/978-3-642-10415-2> (560 pp).
- Richardson, C., Hill, M., Marks, C., Runyen-Janecky, L., Hill, A., 2012. Experimental manipulation of sponge/bacterial symbiont community composition with antibiotics: Sponge cell aggregates as a unique tool to study animal/microorganism symbiosis. *PEMS Microbiol. Ecol.* 81, 407–418. <https://doi.org/10.1111/j.1574-6941.2012.01365.x>.
- Riding, R., 1999. The term stromatolite: towards an essential definition. *Lethaia* 32, 321–330. <https://doi.org/10.1111/j.1502-3931.1999.tb00550.x>.
- Riding, R., 2002. Structure and composition of organic reefs and carbonate mud mounds: concepts and categories. *Earth Sci. Rev.* 58, 163–231. [https://doi.org/10.1016/S0012-8252\(01\)00089-7](https://doi.org/10.1016/S0012-8252(01)00089-7).
- Riding, R., 2006. Microbial carbonate abundance compared with fluctuations in metazoan diversity over geological time. *Sediment. Geol.* 185, 229–238. <https://doi.org/10.1016/j.sedgeo.2005.12.015>.
- Riding, R., 2011. The nature of stromatolites: 3,500 million years of history and a century of research. In: Reitner, J., Quéric, N.-V., Arp, G. (Eds.), Advances in Stromatolite Geobiology, Lecture Notes in Earth Sciences 131. Springer, Heidelberg, pp. 29–74. https://doi.org/10.1007/978-3-642-10415-2_3.
- Riding, R., Awramik, S.M., 2000. *Microbial Sediments*. Springer, Berlin (331 pp).
- Riding, R., Liang, L., Lee, J.-H., Virgine, A., 2019. Influence of dissolved oxygen on secular patterns of marine microbial carbonate abundance during the past 490 Myr. *Palaeogeogr. Palaeoclimatol. Palaeoecol.* 514, 135–143. <https://doi.org/10.1016/j.palaeo.2018.10.006>.
- Rodríguez-Marcoño, S., De la Iglesia, R., Diez, B., Fonseca, C.A., Hajdu, E., Trefault, N., 2015. Characterization of bacterial, archaeal and eukaryote symbionts from antarctic sponges reveals a high diversity at a three-domain level and a particular signature for this ecosystem. *PLoS One* 10, e0138837. <https://doi.org/10.1371/journal.pone.0138837>.
- Rodríguez-Martínez, M., Moreno-González, I., Mas, R., Reitner, J., 2012. Paleoenvironmental reconstruction of microbial mud mound derived boulders from gravity-flow polymictic megabreccias (Viséan, SW Spain). *Sediment. Geol.* 263–264, 157–173. <https://doi.org/10.1016/j.sedgeo.2011.06.010>.
- Ross, R.J., Jaanusson, V., Friedman, I., 1975. Lithology and origin of Middle Ordovician calcareous mudmound at Meiklejohn Peak, southern Nevada, U.S. Geological Survey Professional Paper, p. 48.
- Rützler, K., 1990. Associations between Caribbean sponges and photosynthetic organisms. In: Rützler, K. (Ed.), New Perspective in Sponge Biology: 3rd International Sponge Conference, 1985. Smithsonian Institution Press, Washington, D.C., pp. 455–466.
- Rützler, K., 2012. The role of sponges in the Mesoamerican Barrier-Reef Ecosystem, Belize. In: Becerro, M.A., Uriz, M.J., Maldonado, M., Turon, X. (Eds.), Advances in Sponge Science: Phylogeny, Systematics, Ecology, Advances in Marine Biology 61. Elsevier, pp. 211–271. <https://doi.org/10.1016/B978-0-12-387787-1.00002-7>.
- Schönberg, C.H.L., 2016. Happy relationships between marine sponges and sediments – a review and some observations from Australia. *J. Mar. Biol. Assoc. U. K.* 96, 493–514. <https://doi.org/10.1017/S0025315415001411>.
- Schoop, W.J., 2000. Solution to Darwin's dilemma: discovery of the missing Precambrian record of life. *Proc. Natl. Acad. Sci.* 97, 6947–6953. <https://doi.org/10.1073/pnas.97.13.6947>.
- Scorger, S., Azmy, K., Stouge, S., 2019. Carbon-isotope stratigraphy of the Furongian Berry Head Formation (Port au Port Group) and Tremadocian Watts Bight formation (St. George Group), western Newfoundland, and the correlative significance. *Can. J. Earth Sci.* 56, 223–234. <https://doi.org/10.1139/cjes-2018-0059>.
- Seilacher, A., 1999. Biomat-related lifestyles in the Precambrian. *Palaios* 14, 86–93. <https://doi.org/10.2307/3515363>.
- Semikhatov, M.A., Geblein, C.D., Cloud, P., Awramik, S.M., Benmore, W.C., 1979. Stromatolite morphogenesis—progress and problems. *Can. J. Earth Sci.* 16, 992–1015. <https://doi.org/10.1139/e79-088>.
- Senowbari-Daryan, B., Rigby, J.K., 2011. Part E, revised, volume 4, chapter 7: Sphinctozoan and Inozoan hypercalcified sponges: an overview. In: Treatise Online, vol. 28, pp. 1–90. <https://doi.org/10.17161/to.v0i0.4227>.
- Seppkoski Jr., J.J., 1981. A factor analytic description of the Phanerozoic marine fossil record. *Paleobiology* 7, 36–53. <https://doi.org/10.1017/S0094837300003778>.
- Servais, T., Perrier, V., Danielian, T., Klug, C., Martin, R., Munnecke, A., Nowak, H., Nützel, A., Vandebroucke, T.R.A., Williams, M., Rasmussen, C.M.Ø., 2016. The onset of the 'Ordovician Plankton Revolution' in the late Cambrian. *Palaeoclimatol. Palaeoecol.* 458, 12–28. <https://doi.org/10.1016/j.palaeo.2015.11.003>.
- Seward, A.C., 1931. *Plant Life Through the Ages*. Cambridge University Press, Cambridge (601 pp).
- Shapiro, R.S., Wilmeth, D.T., 2020. Part B, volume 1, chapter 8: microbialites. In: Treatise Online, vol. 134, pp. 1–24.
- Shen, J., Webb, G., 2005. Metazoan-microbial framework fabrics in a Mississippian (Carboniferous) coral-sponge-microbial reef, Monto, Queensland, Australia. *Sediment. Geol.* 178, 113–133. <https://doi.org/10.1016/j.sedgeo.2005.03.011>.
- Shen, Y., Neuweiler, F., 2018. Questioning the microbial origin of automicrite in Ordovician calathid-demosponge carbonate mounds. *Sedimentology* 65, 303–333. <https://doi.org/10.1111/sed.12394>.
- Simion, P., Philippe, H., Baurain, D., Jager, M., Richter, D.J., Di Franco, A., Roure, B., Satoh, N., Queinnec, E., Ereskovsky, A., Lapebie, P., Corre, E., Delsuc, F., King, N., Wörheide, G., Manuel, M., 2017. A large and consistent phylogenomic dataset supports sponges as the sister group to all other animals. *Curr. Biol.* 27, 958–967. <https://doi.org/10.1016/j.cub.2017.02.031>.
- Sperling, E.A., Stockey, R.G., 2018. The temporal and environmental context of early animal evolution: Considering all the ingredients of an "explosion". *Integr. Comp. Biol.* 58, 605–622. <https://doi.org/10.1093/icb/icy088>.
- Stigall, A.L., Edwards, C.T., Freeman, R.L., Rasmussen, C.M.Ø., 2019. Coordinated biotic and abiotic change during the Great Ordovician Biodiversification Event: Darriwilian assembly of early Paleozoic building blocks. *Palaeogeogr. Palaeoclimatol. Palaeoecol.* 530, 249–270. <https://doi.org/10.1016/j.palaeo.2019.05.034>.
- Stock, C.W., Sandberg, C.A., 2019. Latest Devonian (Famennian, *expansa* Zone) conodonts and sponge-microbe symbionts in Pinyon Peak Limestone, Star Range, southwestern Utah, lead to reevaluation of global Dasberg Event. *Palaeogeogr. Palaeoclimatol. Palaeoecol.* 534, 109271. <https://doi.org/10.1016/j.palaeo.2019.109271>.
- Stouge, S., Boyce, D.W., Christiansen, J., Harper, D.A.T., Knight, I., 2001. Vendian – Lower Ordovician stratigraphy of Ella Ø, North-East Greenland: new investigations. In: *Geology of Greenland Survey Bulletin*, vol. 189, pp. 107–114.
- Taylor, M.W., Radax, R., Steger, D., Wagner, M., 2007. Sponge-associated microorganisms: evolution, ecology, and biotechnological potential. *Microbiol. Mol. Biol. Rev.* 71, 295–347. <https://doi.org/10.1128/MMBR.00040-06>.
- Tomás, S., Aurell, M., Bádenas, B., Bjørge, M., Duaso, M., Mutti, M., 2019. Architecture and paleoenvironment of mid-Jurassic microbial-siliceous sponge mounds, Northeastern Spain. *J. Sediment. Res.* 89, 110–134. <https://doi.org/10.2110/jsr.2019.5>.
- Tosti, F., Riding, R., 2017. Fine-grained agglutinated elongate columnar stromatolites: Tieling Formation, ca 1420 Ma, North China. *Sedimentology* 64, 871–902. <https://doi.org/10.1111/sed.12336>.
- Uriz, M.J., Agell, G., Blanquer, A., Turon, X., Casamayor, E.O., 2012. Endosymbiotic calcifying bacteria: a new cue to the origin of calcification in metazoa? *Evolution* 66, 2993–2999. <https://doi.org/10.1111/j.1558-5646.2012.01676.x>.
- Vacelet, J., 1991. Recent Calcarea with a reinforced skeleton ("Pharetroids"). In: Reitner, J., Keupp, H. (Eds.), *Fossil and Recent Sponges*. Springer-Verlag, Berlin Heidelberg, pp. 252–265. https://doi.org/10.1007/978-3-642-75656-6_19.
- Vologdin, A.G., 1962. *The Oldest Algae of the USSR*. Academy of Sciences of the USSR, Moscow (657 pp). (in Russian).
- Walcott, C.D., 1895. Algonkian rocks of the Grand Canyon. *J. Geol.* 3, 312–330. <https://doi.org/10.1086/607191>.
- Walcott, C.D., 1914. Cambrian geology and paleontology III: Precambrian Algonkian algal flora. In: *Smithsonian Miscellaneous Collection*, vol. 64, pp. 77–156.
- Walter, M.R., 1972. Stromatolites and the biostratigraphy of the Australian Precambrian and Cambrian. In: *Special Papers in Palaeontology* 11. The Palaeontological Association (256 pp).
- Walter, M.R., 1976. Stromatolites. In: *Developments in Sedimentology* 20. Elsevier, Amsterdam (790 pp).
- Warnke, K., 1995. Calcification processes of siliceous sponges in Viséan Limestones (Counties Sligo and Leitrim, Northwestern Ireland). *Facies* 33, 215–228. <https://doi.org/10.1007/BF02537453>.
- Weaver, J.C., Aizenberg, J., Fantner, G.E., Kisailus, D., Woesz, A., Allen, P., Fields, K., Porter, M.J., Zok, F.W., Hansma, P.K., Fratzl, P., Morse, D.E., 2007. Hierarchical assembly of the siliceous skeletal lattice of the hexactinellid sponge *Euplectella aspergillum*. *J. Struct. Biol.* 158, 93–106. <https://doi.org/10.1016/j.jsb.2006.10.027>.
- Webb, G.E., 1987. Late Mississippian thrombolite bioherms from the Pitkin Formation of northern Arkansas. *Geol. Soc. Am. Bull.* 99, 686–698. [https://doi.org/10.1130/0016-7606\(1987\)99<686:LMTBFT>2.0.CO;2](https://doi.org/10.1130/0016-7606(1987)99<686:LMTBFT>2.0.CO;2).
- Webby, B.D., 2002. Patterns of Ordovician reef development. In: Kiessling, W., Flügel, E., Golonka, J. (Eds.), *Phanerozoic Reef Patterns*, SEPM Special Publication 72. SEPM, Tulsa, pp. 129–179. <https://doi.org/10.2110/pec.02.72.0129>.
- Webby, B.D., Paris, F., Droser, M.L., Percival, I.G., 2004. *The Great Ordovician Biodiversification Event*. Columbia University Press, New York (497 pp).
- Webster, N.S., Cobb, R.E., Negri, A.P., 2008. Temperature thresholds for bacterial symbiosis with a sponge. *ISME J.* 2, 830–842. <https://doi.org/10.1038/ismej.2008.42>.
- Weidlich, O., 2002. Middle and Late Permian reefs – distributional patterns and reservoir potential. In: Kiessling, W., Flügel, E., Golonka, J. (Eds.), *Phanerozoic Reef Patterns*, SEPM Special Publication 72. SEPM, Tulsa, pp. 339–390. <https://doi.org/10.2110/pec.02.72.0339>.
- Whalan, S., Webster, N.S., 2014. Sponge larval settlement cues: the role of microbial biofilms in a warming ocean. *Sci. Rep.* 4, 4072. <https://doi.org/10.1038/srep04072>.
- Wieland, G.R., 1914. Further notes on Ozarkian seaweeds and oölitites. *Bull. Am. Mus. Nat. Hist.* 33, 237–260.
- Wilkinson, C.R., Cheshire, A.C., 1990. Comparisons of sponge populations across the Barrier Reefs of Australia and Belize: evidence for higher productivity in the Caribbean. *Mar. Ecol. Prog. Ser.* 67, 285–294. <https://doi.org/10.3354/meps067285>.
- Williams, H., James, N.P., Stevens, R.K., 1985. Humber Arm allochthon and nearby groups between Bonne Bay and Portland Creek, western Newfoundland. In: *Current research, Part A, Geological Survey of Canada*, pp. 399–406.
- Wood, R., 1990. Reef-building sponges. *Am. Sci.* 78, 224–235.
- Wood, R., 1999. *Reef Evolution*. Oxford University Press, Oxford (414 pp).
- Wood, R., Penny, A., 2018. Substrate growth dynamics and biomineralization of an Ediacaran encrusting poriferan. *Proc. R. Soc. B* 285, 20171938. <https://doi.org/10.1098/rspb.2017.1938>.

- Wörheide, G., 2008. A hypercalcified sponge with soft relatives: *Vaceletia* is a keratose demosponge. Mol. Phylogenet. Evol. 47, 433–438. <https://doi.org/10.1016/j.mpev.2008.01.021>.
- Wörheide, G., Dohrmann, M., Erpenbeck, D., Larroux, C., Maldonado, M., Voigt, O., Borchellini, C., Lavrov, D.V., 2012. Deep phylogeny and evolution of sponges (phylum Porifera). In: Beccero, M.A., Uriz, M.J., Maldonado, M., Turon, X. (Eds.), Advances in Marine Biology 61. Academic Press, Amsterdam, pp. 1–78. <https://doi.org/10.1016/B978-0-12-387787-1.00007-6>.
- Yang, X., Zhao, Y., Babcock, L.E., Peng, J.I.N., 2017. A new vauxiid sponge from the Kaili Biota (Cambrian Stage 5), Guizhou, South China. Geol. Mag. 154, 1334–1343. <https://doi.org/10.1017/s0016756816001229>.
- Yao, L., Aretz, M., Wignall, P.B., Chen, J., Vachard, D., Qi, Y., Shen, S., Wang, X., 2020. The longest delay: Re-emergence of coral reef ecosystems after the Late Devonian extinctions. Earth Sci. Rev. 203, 103060 <https://doi.org/10.1016/j.earscirev.2019.103060>.
- Yin, Z., Zhu, M., Davidson, E.H., Bottjer, D.J., Zhao, F., Tafforeau, P., 2015. Sponge grade body fossil with cellular resolution dating 60 Myr before the Cambrian. Proc. Natl. Acad. Sci. 112, E1453–E1460. <https://doi.org/10.1073/pnas.1414577112>.
- Zhou, K., Pratt, B.R., 2019. Composition and origin of stromatactis-bearing mud-mounds (Upper Devonian, Frasnian), southern Rocky Mountains, western Canada. Sedimentology 66, 2455–2489. <https://doi.org/10.1111/sed.12595>.